

## CLIMATOLOGY

## Morphological consequences of climate change for resident birds in intact Amazonian rainforest

Vitek Jirinec<sup>1,2\*</sup>, Ryan C. Burner<sup>3†</sup>, Bruna R. Amaral<sup>2,4,5</sup>, Richard O. Bierregaard Jr.<sup>2</sup>, Gilberto Fernández-Arellano<sup>2,4,6</sup>, Angélica Hernández-Palma<sup>1,2,7</sup>, Erik I. Johnson<sup>1,2,8</sup>, Thomas E. Lovejoy<sup>2,9</sup>, Luke L. Powell<sup>1,2,10,11</sup>, Cameron L. Rutt<sup>1,2,12</sup>, Jared D. Wolfe<sup>1,2,11,13</sup>, Philip C. Stouffer<sup>1,2</sup>

Warming from climate change is expected to reduce body size of endotherms, but studies from temperate systems have produced equivocal results. Over four decades, we collected morphometric data on a nonmigratory understory bird community within Amazonian primary rainforest that is experiencing increasingly extreme climate. All 77 species showed lower mean mass since the early 1980s—nearly half with 95% confidence. A third of species concomitantly increased wing length, driving a decrease in mass:wing ratio for 69% of species. Seasonal precipitation patterns were generally better than temperature at explaining morphological variation. Short-term climatic conditions affected all metrics, but time trends in wing and mass:wing remained robust even after controlling for annual seasonal conditions. We attribute these results to pressures to increase resource economy under warming. Both seasonal and long-term morphological shifts suggest response to climate change and highlight its pervasive consequences, even in the heart of the world's largest rainforest.

## INTRODUCTION

Human-caused climate change is one of the key agents of ecosystem transformation in the Anthropocene (1, 2), yet inadequate sampling obscures its impacts in tropical biodiversity hotspots (3, 4). Assessing the consequences of climate change requires long-term monitoring of populations, data that are available for some plants (5, 6) but are rare for vertebrates. For birds, which are good indicators of environmental change (7), limited datasets are available in the Neotropics, where birds reach the peak of their global diversity (8). Amazonia, the world's largest tropical forest, is represented by two such datasets—in Brazil and Ecuador—both of which have recently revealed substantial abundance declines in multiple species over several decades within intact rainforest experiencing little to no local disturbance (9, 10). Given the absence of apparent local stressors, regional trends in temperature and rainfall (11), and theoretical support that tropical species are especially sensitive to environmental change (12, 13), these findings raise the possibility that

climate change is altering the avifauna in the vast rainforests of lowland Amazonia.

Are birds responding to climate change? Trends in abundance, coupled with large-scale climate patterns, provide one line of correlative evidence. Another postulated response to climate change—and warming especially—is reduction of body size (14). This expectation often stems from Bergmann's rule for latitudinal variation whereby individuals tend to be smaller at lower latitudes (15, 16). Up to 76% of birds follow this pattern, particularly sedentary species (17). Although Bergmann originally framed the rule as heat conservation with lower body surface:volume ratio in cooler climates (18), its corollary applies to heat loss in warm and warming conditions (14). This led to the expectation that, along with shifts in distribution (19) and phenology (20), decreasing body size could be the third universal response to warming (21). Yet, studies reported both decreasing and increasing body sizes in birds through time (14, 22). This lack of consistency may stem from the focal systems to date—birds almost exclusively at temperate latitudes, in landscapes that were often altered, and primarily migratory species. In these systems, the effects of warming are challenging to disentangle from competing pressures on bird morphology. For example, smaller bird size was associated with habitat degradation (23) while wild landscapes are increasingly transformed for anthropogenic use (24). For migratory birds, shifts in distribution and phenology may affect individuals observed at a specific monitoring point, while links to climate are further complicated by the fact that migrants are exposed to conditions in a wide (and often unknown) geographic area with possibly disparate climate trends (25). Still, remarkably consistent decreases in body size were detected in a large dataset of migratory birds passing through Chicago (USA) with reduction evident in several metrics of body size across 52 species (26). Reductions were correlated with broadly increasing summer temperatures. Curiously, however, wing length also concurrently increased in most species, a phenomenon interpreted as compensatory offset for smaller size to maintain migration (26). Current knowledge thus indicates a shift in body size and shape in a diverse and widely

<sup>1</sup>School of Renewable Natural Resources, Louisiana State University and LSU AgCenter, Baton Rouge, LA 70803, USA. <sup>2</sup>Biological Dynamics of Forest Fragments Project, Instituto Nacional de Pesquisas da Amazônia (INPA), Manaus, Amazonas, Brazil. <sup>3</sup>Faculty of Environmental Sciences and Natural Resource Management, Norwegian University of Life Sciences, 1435 Aas, Norway. <sup>4</sup>Department of Ecology, Instituto de Biociências, Universidade Federal do Rio Grande do Sul, Porto Alegre, Brazil. <sup>5</sup>Department of Ecosystem Science and Management, Pennsylvania State University, University Park, PA 16802, USA. <sup>6</sup>Departamento de Botânica e Ecologia, Universidade Federal de Mato Grosso, Cuiabá, Brazil. <sup>7</sup>Instituto de Investigación de Recursos Biológicos Alexander von Humboldt, Avenida Paseo Bolívar 16-20, Bogotá, Colombia. <sup>8</sup>National Audubon Society, 5615 Corporate Blvd., Baton Rouge, LA 70808, USA. <sup>9</sup>Department of Environmental Science and Policy, George Mason University, Fairfax, VA 22030, USA. <sup>10</sup>CIBIO-InBIO, Research Centre in Biodiversity and Genetic Resources, University of Porto, Campus de Vairão, 4485-661 Vairão, Portugal. <sup>11</sup>Biodiversity Initiative, Houghton, MI 49931, USA. <sup>12</sup>Department of Biology, George Mason University, Fairfax, VA 22030, USA. <sup>13</sup>College of Forest Resources and Environmental Science, Michigan Technological University, Houghton, MI 49931, USA.

\*Corresponding author. Email: vjirine1@lsu.edu

†Present address: U.S. Geological Survey, Upper Midwest Environmental Sciences Center, 2630 Fanta Reed Road, La Crosse, WI 54603, USA.

distributed group of migratory birds, a pattern consistent with expectations under climate warming. However, the broad breeding and wintering distributions of the species sampled, coupled with landscape change on the breeding and wintering grounds, make it difficult to assess how climatic conditions align with morphological change.

Conversely, primary forests in equatorial lowlands of Amazonia hold an avifauna that consists almost exclusively of year-round resident species not subject to demands of migration, ingressions of individuals from other regions or elevations, or, in some settings, landscape disturbance. In this system, the link between bird morphology and climate can be explicitly evaluated under known conditions throughout the measurement time series. Furthermore, estimated abundance trends of the same populations from an earlier study (9)—including the role of ecological traits—provide a rare opportunity to leverage abundance trends to test for the adaptive capacity of morphological shifts under climate change. South America faces the greatest extinction risks due to climate change (27), in part because resident species in equatorial lowlands—often with small ranges delineated by rivers (28)—are not equipped to adapt to changing conditions through distant latitudinal or elevational shifts (29). For these species, population trends are likely proportional to their adaptive capacity (either through microevolution or plasticity) to respond to unusual conditions (30). Here, we test for climate-related reduction in body size in a community of understory birds in intact rainforests of central Amazonia. We then compare morphological shifts with abundance trends across four decades, expecting less morphological change in species with higher abundance declines.

## RESULTS

First, we used >50 years of model-based reanalyses of climate data to quantify in situ climate trends at the Biological Dynamics of Forest Fragments Project (BDFFP) in Brazilian Amazonia, where birds were sampled (Fig. 1A). We found that, since 1966, mean precipitation increased by 13% in the wet season and fell by 15% in the dry season (Fig. 1B). In contrast, mean temperature increased linearly in both seasons, with temperatures increasing by 1.00°C in the wet season and 1.65°C in the dry season (Fig. 1B). These results represent climate change that overlaps spatiotemporally with our bird morphometric data.

We then compiled measurements of body mass ( $n = 14,842$  individuals), wing length ( $n = 11,582$  individuals), and of mass-to-wing ratio ( $n = 11,009$  individuals) for 77 resident bird species from 22 families captured over 40 years across 43 km of primary terra firme forest. Birds were sampled within undisturbed, unfragmented primary forest in a landscape that remained >90% forested overall (31). We used body mass to represent body size (26), but we also included wing length and mass-to-wing length ratio (mass:wing) to help resolve the role of factors unrelated to size, such as body shape and condition (26, 32). If morphological change represents adaptation to climate change, we hypothesized that morphology and abundance would be correlated. We analyzed morphological data using hierarchical Bayesian joint species models that incorporated effects of traits and phylogenetic relationships (33) and conducted a parallel analysis with linear mixed models (LMMs) without traits and phylogeny. We found declines in mass across the community: 95% Bayesian credible intervals (CIs) for the effect of year on

mass were entirely negative for 36 (47%) species, thus providing strong evidence that these birds decreased in mass—up to 1.8% per decade of their baseline mass in 1980 (Fig. 1, C and D). Moreover, our results indicated with at least 90% probability that 44 (57%) species declined in mass, with all 77 examined species showing mean decreases. Accompanying mass changes, 61 (79%) species showed mean increases in wing length through time, with 22 (30%) having 95% CIs that were entirely positive (Fig. 1, C and D). Only one species—a hummingbird—had a negative wing trend at 95% probability. Community-wide reduction in mass coupled with a general increase in wing length resulted in widespread decreases in mass:wing over time, with 53 (69%) and 60 (78%) species having 95% and 90% CIs, respectively, that were entirely negative (Fig. 1, C and D). All 77 species showed mean reduction in mass:wing. These morphological shifts did not differ across foraging guilds, despite guild-linked differences in abundance trends. Terrestrial and near-ground insectivores declined in abundance (9) but did not undergo more morphological change relative to other guilds (fig. S1). Overall, we found no relationship between abundance and morphology (fig. S2), and all 12 foraging guilds showed broadly comparable morphological changes in our phylogenetically informed analyses (fig. S1). However, models identified vertical niche as an important factor—mass:wing 95% CIs were entirely negative for midstory species (Fig. 2 and fig. S1). LMMs were congruent with the Bayesian analysis—mass and mass:wing have decreased, while wing has increased through time across the community (table S1).

Next, we tested for relationships between morphology and variation in rainfall and temperature during the season of bird sampling and at two time lags. We found robust links between bird mass and seasonal climate (Figs. 3 and 4). Time trend (year) in mass disappeared after controlling for lagged temperature (Fig. 3A). Time trend remained after controlling for lagged precipitation for mass and for wing and mass:wing ratio after controlling for either temperature or precipitation (Fig. 3, B to F). Birds were lighter when hotter and drier conditions occurred during the season of measurement (dry season; lag 0), but this relationship was even stronger at lag 2—conditions in the dry season of the preceding year (Fig. 3, A and D). The inverse was true for the effect of lag 1, with heavier birds after the previous wet season was hotter and drier (Fig. 3, A and D). The general effect of climate was similar for wing length—although lag 0 CIs overlapped zero, birds were shorter-winged with hotter and drier dry seasons at lag 2, and longer-winged after hotter and drier wet seasons (Fig. 3, B and E). The effect of seasonal variation on mass:wing generally matched mass and wing, but most species declined with year even after controlling for lagged temperature and precipitation (Figs. 3 and 4). As in year-only models, bird morphology did not vary by foraging guild in climate models (fig. S3), but temporal declines in mass:wing remained for species in the midstory stratum after controlling for lagged climate (fig. S4). As in the year-only analysis, LMMs agreed with Bayesian joint species models (fig. S5 and tables S2 and S3).

Precipitation models performed better than temperature models. Temperature and precipitation were modeled separately because they were highly inversely correlated. In the nine cases where we examined the separate effect of precipitation and temperature on morphology using identical model structures, coefficient of determination ( $R^2$ ) was higher in the equivalent precipitation model (table S4). In the parallel analysis with LMMs with climate covariates (tables S2 and S3), precipitation models of mass, wing, and mass:wing had

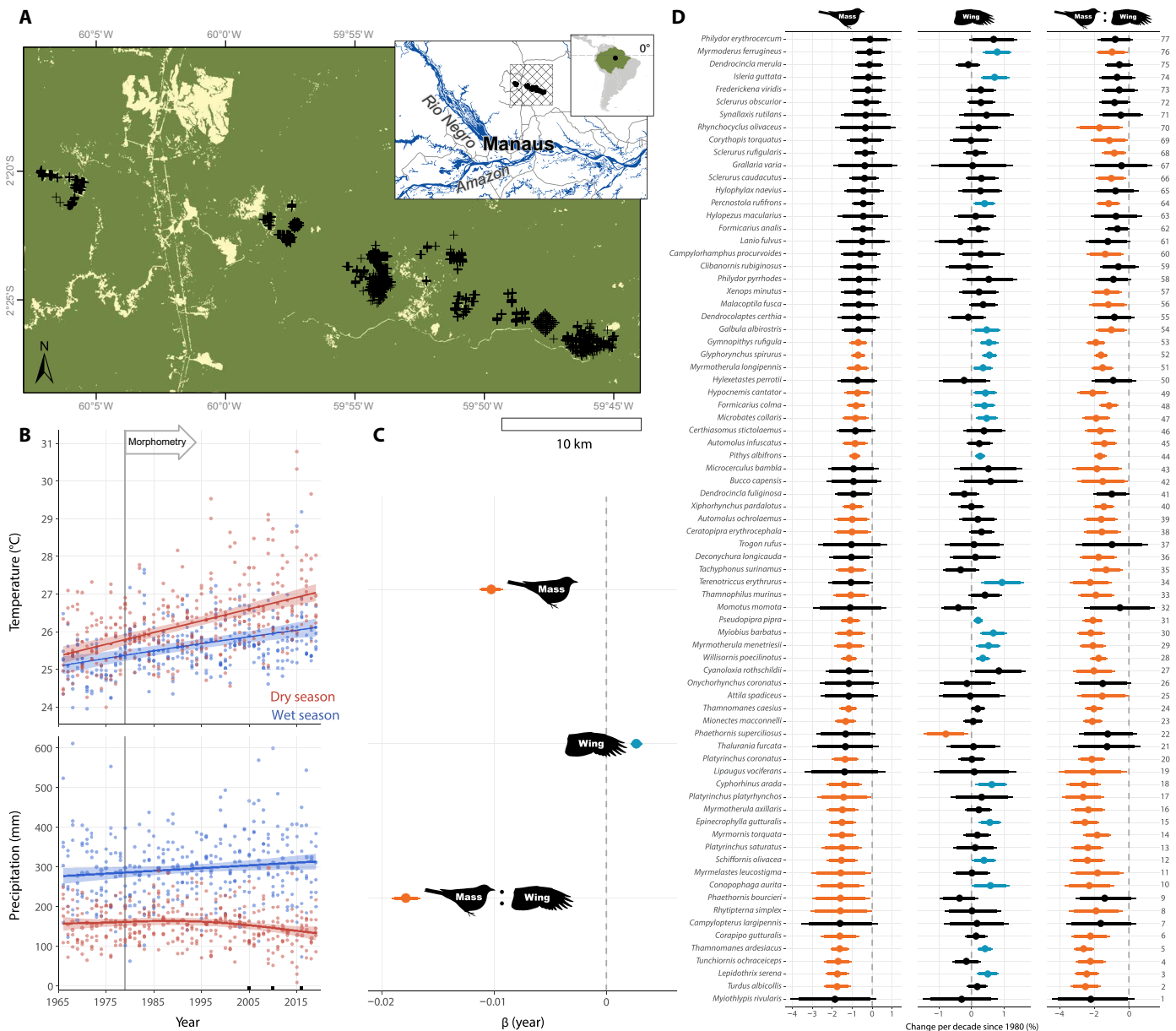


**Fig. 1. Bird body change and climate trends within undisturbed Amazonia.** (A) Capture locations (crosses) in primary forest within the Amazon rainforest ecoregion, showing forest extent in 2020 derived from Landsat 8 imagery (map includes sites sampled before forest clearing). (B) Mean temperature and total precipitation (points) per season using climate reanalysis tiles [crosshatch in (A) inset] overlapping capture data. Lines and confidence intervals are outputs from generalized additive mixed models showing in situ climate change. Black squares on the x axis highlight recent widespread droughts (82–84). (C) Mass, wing length, and mass:wing ratio trends of 77 bird species measured in 1979–2019. To obtain overall trend, species were pooled and designated as a random effect in Bayesian hierarchical models. Points are medians with 90% and 95% credible intervals (CIs). Estimates are colored orange if 95% CIs are entirely negative, blue if entirely positive, or black if overlapping zero. Results correspond to models 19, 22, and 25 (table S4). (D) Morphological trends of individual species, ordered by declining mass. Numbers on the right correspond to the same species in Fig. 4. Results correspond to models 1, 7, and 13 (table S4).

Akaike information criterion (AIC) values lower by 27.6, 19.0, and 6.1 units relative to the equivalent temperature model.

**DISCUSSION**

Community-wide declines in mass follow the expectation of smaller body sizes under warming climate and suggest that even understory birds in lowland tropical forests are responding to a changing environment.

In endotherms, birds are more exposed to climate change than mammals (34), and tropical birds are theoretically most vulnerable according to Janzen’s seasonality hypothesis (13, 35). The temporal analog of Bergmann’s rule for latitudinal variation indicates that smaller body size is favored under warming world (14), especially given strong, negative correlations of body size with wet-bulb temperature (36). Over four decades at our equatorial site, birds experienced gradually warmer temperatures throughout their annual cycle (Fig. 1B).

Downloaded from https://www.science.org on November 12, 2021

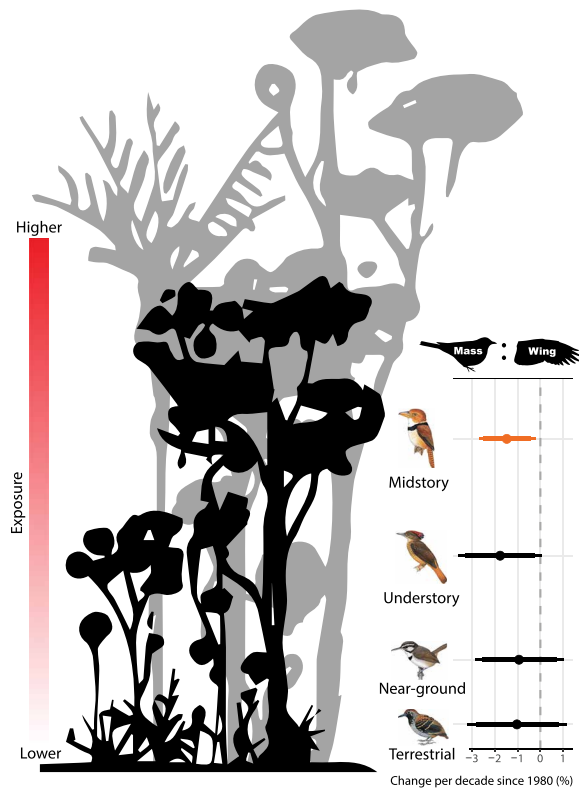


**Fig. 2. Mass:wing ratio trend by forest vertical niche.** Points are median estimates from the second level (trait) of Bayesian hierarchical models shown in Fig. 1D, with lines representing 90% and 95% CIs. Out of the three morphological metrics, only mass:wing ratio for midstory species had 95% CIs that did not overlap zero for the guild as a whole. Estimates are colored orange if 95% CIs are entirely negative, blue if entirely positive, or black if overlapping zero. Relative to the buffered microclimate on the forest floor, upper-stratum conditions are generally more severe (53,85). Results correspond to model 16 (table S4).

Time-trend models of mass indicated that all 77 species decreased in mean mass, with nearly half the sampled community declining at 95% probability (Fig. 1D). However, the effect of the time trend on mass largely disappeared after controlling for lagged temperature (Fig. 3A), matching another study that included lagged climate covariates (37). This suggests that bird mass is linked to shorter-term fluctuations in climatic conditions, and an increasingly extreme environment thus results in lighter birds over time. Notably, we found that the effects of climate on morphology generally differed by seasonal lags (Figs. 3 and 4). Because the seasonal cycle is itself defined by precipitation and temperature (i.e., less precipitation and higher temperature in the dry season and vice versa), the result that mass increased not only after cooler, wetter dry seasons but also after hotter, drier wet seasons signals that intermediate conditions are indeed optimal for tropical birds, as the seasonality hypothesis posits (35). Directional climate change—particularly hotter and drier dry seasons (Fig. 1B)—was associated with lighter birds, but extremes in either season appear to contribute to the observed morphological trends.

Unlike decreasing mass, elongating wings are more difficult to explain using existing theory. Longer wings are interpretable as a temporal analog of Allen's rule (38), where pronounced body extremities better offload heat, but this explanation assumes that

longer wings reflect longer wing bones, rather than simply longer feathers (which do not dissipate heat). Some studies have considered wing length a measure of body size (39), but wing size and shape are also inextricably linked to flight performance (40). Near-universal declines in several metrics of body size (including mass) were documented in a large sample of birds collected during migration (26), but these populations showed similarly consistent increases in wing length. Longer wings were interpreted as compensation for demands of migration with smaller bodies, but here we observed the same phenomenon in birds that do not migrate. A related hypothesis for elongating wings in Amazonian residents is that changing landscape configuration (e.g., more natural gaps or anthropogenic disturbance) pushes birds to fly more frequently, when more pointed wings could be advantageous (40). However, this is generally inconsistent with the fact that BDFFP forest cover has increased over the study interval (31), thus diminishing the need for possible long-distance crossing of nonforest areas. We sampled within vast areas of primary forest, and most birds are likely to spend their entire lives within this local setting. Moreover, substantial movement across the small proportion of disturbed landscape is unlikely to occur in our system—research from lowland forest in Panama (41) as well as our site (42) indicates that many understory species are unwilling to cross nonhabitat areas. Our dataset broadly overlaps with Stouffer *et al.* (9), which showed that under our protocols, bird capture rates and local bird community composition did not change with distance to forest edge. Conversely, community composition differed substantially in disturbed forest—both among sites and relative to undisturbed forest. These results do not support more frequent flight in our system owing to anthropogenic disturbance at the landscape scale, but the role of more subtle changes of forest structure or composition within primary forest should be considered in future studies.

Compared with temperature effects, the role of precipitation is seldom considered in temporal studies of bird size. Yet, water appears to play an important role, at least in combination with temperature (36). Precipitation models fit better relative to analogous models with temperature covariates—in every instance, precipitation models explained more variation in morphology than temperature. Precipitation models outperformed temperature in our main Bayesian analysis regardless of whether we incorporated effects of phylogeny and species traits (table S4), and similar results emerged in the parallel LMMs (tables S2 and S3). These findings support a recent review that highlights the importance of hygric niches for tropical endotherms (43), as well as the role of precipitation in bird adaptive capacity (30). The relationship between water availability and body size could be indirect, such as when drier conditions reduce insect or fruit resources. In addition, because physiological thermoregulation of endotherms is inextricably linked with water availability (12), diminished access to water may have direct consequences for birds, especially when mixed with thermal stress. Notably, precipitation shifts in the tropics under anthropogenic climate change are more spatially variable than a more consistent warming trend (44, 45). If rainfall indeed plays a prominent role in avian morphology, then this spatial heterogeneity may explain the inconsistency in temporal size trends (22), especially given that many of the migratory species examined spend most of their lives on the wintering grounds across the Neotropics.

Yet, the pattern in the three metrics of body change taken together is consistent with the expectation of maintaining flight efficiency



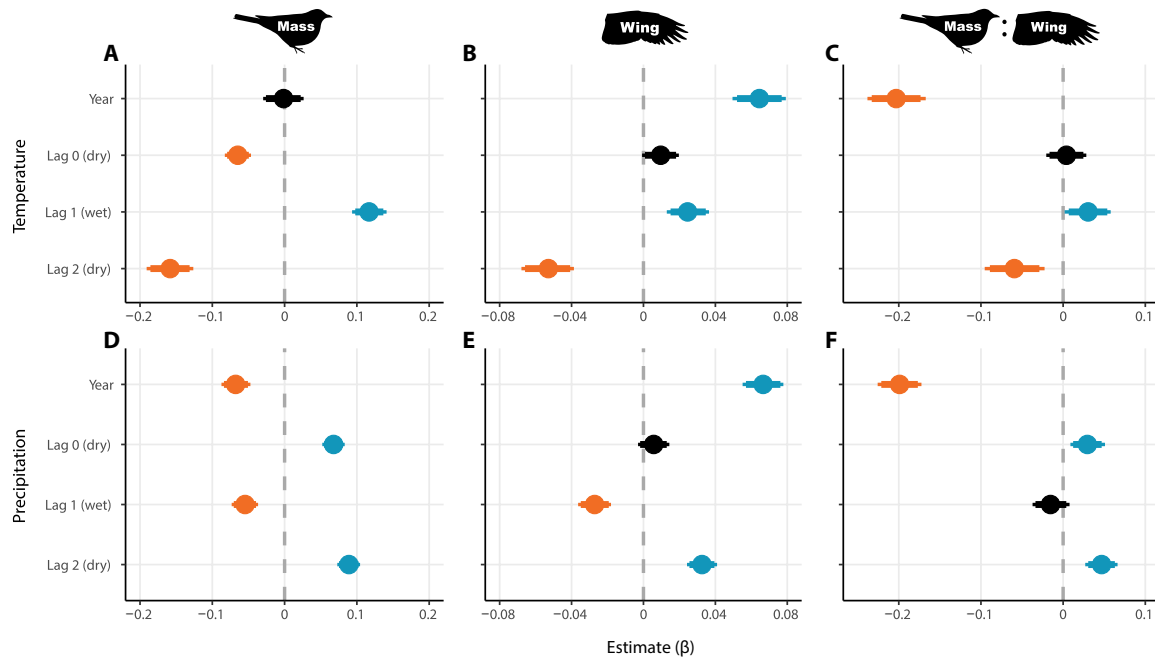


**Fig. 3. Bird morphology modeled by time trend and climate covariates.** Each panel shows parameter estimates of a single model for one of the three metrics representing bird morphology in the community as a whole as response (columns), and time trend (year) and temperature (A to C) or precipitation (D to F) as covariates. Lag 0 is the season of capture (dry season), with lags 1 and 2 the previous wet and dry seasons, respectively. Points are medians with 90% and 95% CIs. Estimates are colored orange if 95% CIs are entirely negative, blue if entirely positive, or black if overlapping zero. Results correspond to models 20, 21, 23, 24, 26, and 27 (table S4).

under either resource shortage or thermal stress. Assuming no change in wing shape, mass:wing is proportional to wing loading (mass:wing area) and minimizing wing loading lowers caloric demand of flight and thus metabolic heat production (fig. S6)—an adaptive strategy under directional selection by resource scarcity or warming, but also a trade-off for lower flight speeds (46). Moreover, resource shortage and thermal stress are coupled if both higher energy and water requirements (12) that accompany dry seasons are becoming increasingly pronounced (Fig. 1B). Decreasing mass and increasing wing length may be the most economic strategy to reduce wing loading (fig. S6), and our results align with this explanation. Individual-level decreases in mass:wing were more prevalent (69% of species) in our community than decreases in mass (47%) and increases in wing (30%), the latter two of which are population-level metrics that were not correlated (fig. S7).

Are these morphological changes evolutionary responses to a shifting environment? Climate change can evidently exert directional selection (47), but obtaining unequivocal evidence of microevolution is very challenging as it requires genomic or quantitative genetic approaches (47), methods that are impractical for many wild populations (14). Consequently, studies claiming microevolution as a mechanism for observed temporal size clines often cannot separate genetic response from phenotypic plasticity (48), which may be modulated by complex epigenetics (49). Still, evolutionary consequences of environmental change on bird morphology have been documented over a shorter interval than we present in this study (50) and were linked to climate change explicitly (30). Aside from an adaptive outcome under increasing temperatures, declines in mass may be caused by nutritional strain. Mass was negatively associated with more extreme dry seasons (Figs. 3 and 4), raising the

possibility that bird condition fell in stressful years with lower food availability. However, morphological shifts arose across foraging guilds and were similar in terrestrial insectivores and midstory frugivores (fig. S1), even though these groups had diametrically opposed trends in relative abundance over the same interval (9). Furthermore, we saw many declining-mass species with concomitant wing increases—a conflicting outcome under the assumption of unfavorable conditions (51). Lagged effects of temperature and precipitation on wing length aligned with the outcome expected owing to stress—both lower mass and shorter wings after hotter and drier dry seasons, but for many species, wings elongated through time even after controlling for climate (Figs. 3 and 4). In mass:wing models, year was the most important variable with seasonal climate contributing little, a pattern consistent with both parameter coefficients and model fit (Figs. 3 and 4 and tables S1 to S4). Because the time trend for mass—but not for wing and especially not for mass:wing—mostly faded after controlling for seasonal temperature, it is possible that lower bird mass is a plastic response to changing climate whereas lower mass:wing and longer wings are an adaptive compensation with a yet unresolved mechanism.

Another explanation for shifting morphology may be changes in age ratios if morphology differs by age groups. Addressing this possibility is complicated by the fact that skill to age tropical species has itself increased over time, only recently reaching a level that allows many species to be reliably aged (52). We used latest knowledge and capture notes to classify captures into age groups where possible and found that all three morphological metrics were lower in juveniles (table S5). Because we found not only broadly decreasing mass but also increasing wing length across most species through time, our results do not appear to be driven by changes in age ratios.

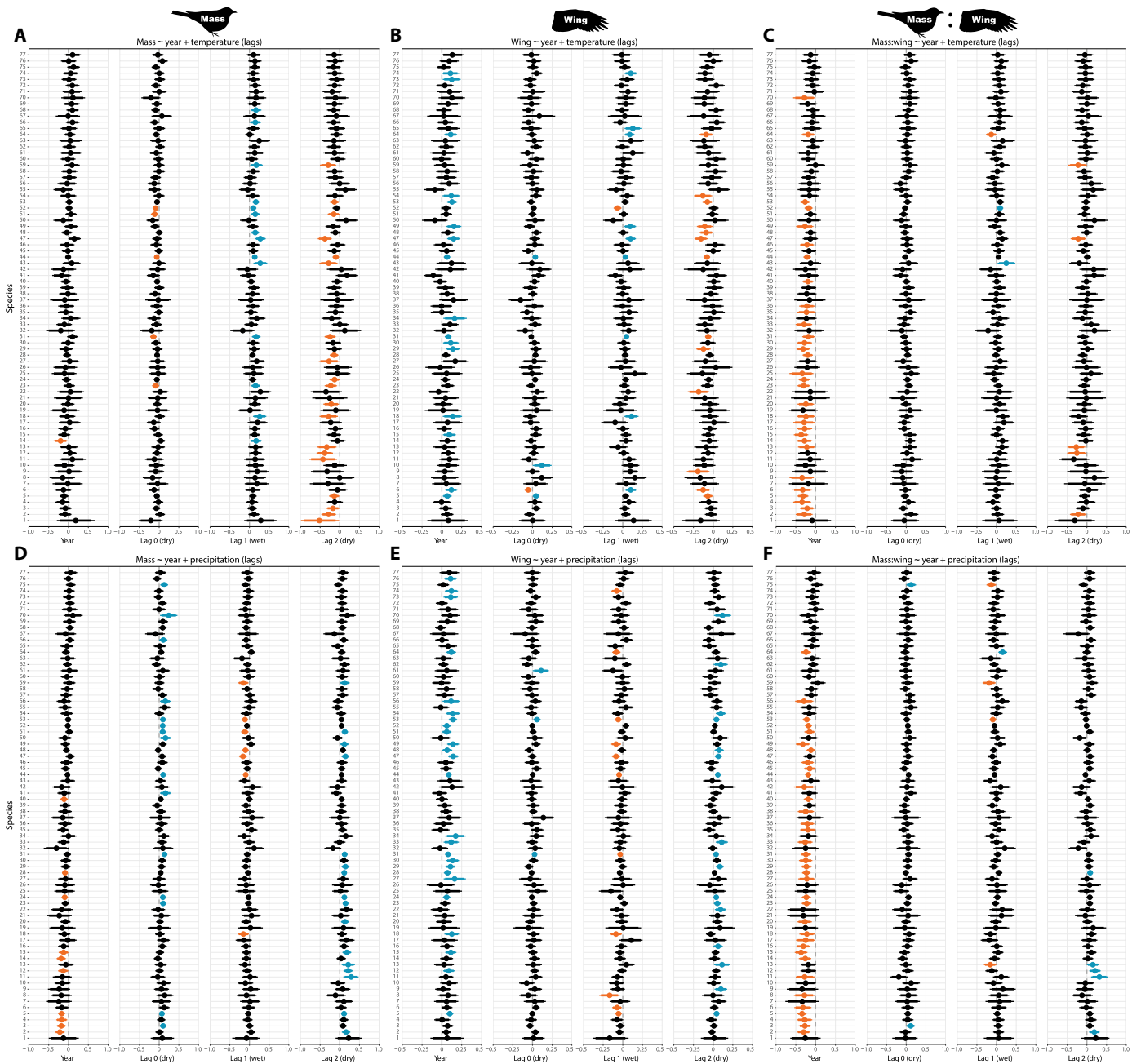


**Fig. 4. Morphology by species modeled by time trend and climate covariates.** (A to C) Models of bird morphology metrics by year and mean temperature during the season of capture (dry season—lag 0) and two seasonal lags (previous wet—lag 1 and previous dry—lag 2). (D to F) Models of bird morphology by year and total precipitation. Species are ranked by declining mass (Fig. 1D), with points showing medians with 90% and 95% CIs estimated with Bayesian hierarchical models. Estimates are colored orange if 95% CIs are entirely negative, blue if entirely positive, or black if overlapping zero. Results correspond to models 2, 3, 8, 9, 14, and 15 (table S4).

Morphological change varied little with ecological traits, including traits strongly associated with long-term abundance trends in undisturbed forest (9). We found little correlation between abundance and morphology trends (fig. S2). Thus, if at least some morphological shifts are adaptive, trait-linked abundance trends may be the result of trait-linked ecological factors. Out of all ecological traits, the only case where species sharing a trait showed a consistent change (95% CIs) was declining mass:wing for midstory

species (fig. S1). This result may represent more evidence for the role of temperature as the driver of morphological change, because birds of higher forest strata are more exposed to increasing temperatures (Fig. 2), while they also rely heavily on flight compared to less volant species on or near the ground. Apparent abundance increases of higher-stratum species over decades revealed through capture rates in understory mist nets (9) could reflect a shift of upper understory species to cooler niches below, as suggested by

Downloaded from https://www.science.org on November 12, 2021

observations throughout the diurnal cycle (53). Subsequently greater spatial overlap with upper-stratum species on top of abiotic climate shifts may affect demographic parameters of terrestrial and near-ground species even though they inhabit the most buffered of environments (13, 54). Capture rates of these species should not be biased by climate change, and increased temperature was negatively associated with demographic rates in an Afrotropical bird community (55), a finding consistent with population trends in these well-sampled guilds. Alternatively, specialization to the microclimatic consistency of the rainforest floor—as suggested by the seasonality hypothesis and supported by sensitivity of terrestrial and near-ground insectivores to forest clearing and fragmentation (56)—may also confer little capacity for an adaptive morphological response, regardless of whether it stems from plasticity or microevolution.

Faced with a changing environment, biological responses of species are limited to extinction, distribution shifts, and adaptation. For birds in lowland Amazonia, population trends for a subset of the community are not encouraging (9, 10), and tracking shifting conditions through space would require moving very large distances (29) across South American rivers, which form often insurmountable barriers (28). Here, we show that the body size of a large part of Amazonian avifauna shifted through time with remarkable consistency across this diverse community of resident birds. Our study matches recent results for migratory birds where elongating wings were interpreted to aid migration with smaller body sizes (26). Because we detected the same patterns in species that do not undertake extensive flights, we suggest that a more parsimonious explanation is resource economy (water and energy) under warming climate. Bird morphology is transforming toward lighter bodies and longer wings, with reductions in mass:wing ratio particularly prevalent. Short-term fluctuations in seasonal climate—and precipitation especially—appear to drive chiefly the variation in mass, and less so in wing and mass:wing. Together, body proportions moved in the direction of more efficient flight and lower metabolic heat production and are consistent with a plastic or genetic adaptation to resource or thermal stress under climate change. Regardless of the mechanism behind these changes, bird morphology reveals the sensitivity of Amazonian biota to global human activity, even in the absence of local stressors like deforestation. Temperate regions maintain monitoring programs that enable tracking of Anthropocene's impacts at the large scale (57). Our results suggest that equivalent efforts are warranted for the most speciose group of vertebrates at the core of their diversity.

## MATERIALS AND METHODS

### Study site

Mass and wing measurements were collected from 1979 to 2019 at the BDFFP, in Amazonas, Brazil, located ~70 km north of Manaus (2° 24' 21" S, 59° 52' 25" W). Bird sampling was regular throughout the four decades, but data gaps inevitably occurred because of lapses in funding and captures thus come from fewer years ( $n = 26$  years). Although assessing the effects of landscape disturbance was the primary motivation for establishing the BDFFP in the late 1970s, the area remained embedded in a vast expanse of undisturbed rainforest—forest cover persisted at >90% within 10 km around experimental reserves (31). Throughout the years, birds were sampled in continuous primary forest far from human disturbance as well as at disturbed sites—forest fragments and secondary forest (58). Here, we remove

any effects of landscape change by only including data from undisturbed forest at the BDFFP. We emphasize that despite the acronym, the BDFFP area consists mainly of primary forest.

### Bird data

Birds were captured in mist nets using standardized protocols (58). Net type was identical throughout the sampling period—38-mm mesh size, with dimensions of 12 m by 2.5 m. Nets were generally placed in a single line of 16, but the number of nets and configuration varied. Most birds were caught with passive netting with nets open between 06:00 and 14:00 local time, but a subset of captures (16%) come from nets closed at 12:00. Terrestrial insectivores are seldom captured with passive netting because of their ambulatory locomotion, and this ecological guild has become rare in recent years (9) and thus of particular interest in this study. For a sufficient sample for terrestrial insectivores, we included birds lured into nets with playback in 2017–2019 (59), with captures throughout the day. Although some temperate birds may weigh less in the morning (60, 61), the inclusion of potentially heavier individuals obtained by target netting (i.e., with some measured late in the afternoon) would work contrary to the predicted lower mass in the latter years.

Captured birds were identified, processed, and released. Processing included marking with an alphanumeric leg band and measuring of wing length and body mass. Method for taking wing length remained unchanged for all birds—using an end-stop ruler, observers measured wing chord (i.e., length with natural wing curvature) from the carpal joint to the tip of the longest primary to the nearest 1 mm. However, for mass, equipment improvements led to a shift from analog spring scales (Pesola; Feusisberg, Switzerland), often at a resolution of 0.25 or 0.5 g, to electronic balances (usually manufactured by Ohaus; Parsippany, NJ, USA), with a resolution of 0.1 g. Relatively lower mass resolution was unlikely to lead to systematically higher records of early mass. Animal care protocols were authorized by Centro Nacional de Pesquisa e Conservação de Aves Silvestres (CEMAVE) and IBAMA (CNPq Processo EXC 021/06-C) in Brazil and Louisiana State University (IACUC A2006-02).

For analysis, we selected bird records in a way that removed the influence of land cover change and seasonal sampling bias. First, we excluded captures from fragments and secondary forest. Then, to reconcile unequal seasonal sampling in recent years, we restricted captures to the dry season (June through November). We further filtered birds to first captures of each individual and excluded species with fewer than five records of either mass or wing before or after the median year (2000). Records missing both mass and wing measurements, or with mass or wing measurements greater or less than 4 SD from the mean value for the species, were considered as errors (identification or measurement) and dropped. This process yielded measurements for 15,415 individuals of 77 species (mass,  $n = 14,842$ ; wing,  $n = 11,582$ ; mass:wing,  $n = 11,009$ ).

Bird bodies can vary by age, sex, breeding condition, and molt status. However, we treated all of these categories equally in the analysis for several reasons. Sex can only be determined for some species because many are sexually monochromatic (52). Although a subset of species and individuals can be reliably aged, aging characteristics fade soon after fledging for many species (52), and recent advances in aging techniques were not available in the early years of data collection and thus age filtering could bias the sample. Nevertheless, to understand the general effect of age on morphology in our system, we reassigned molt cycles to binary “adult” and “juvenile” groups

where possible and tested for group effects (table S5). Breeding status can also influence bird mass via inclusion of gravid females or energetic demands on either sex with an active nest; however, in contrast to temperate-breeding birds, species at our site generally nest throughout the year (62), thus breeding season cannot be broadly controlled for within models by inclusion of breeding months, etc. Wing length can be underestimated in molting individuals, but these species also molt throughout the year (63). Furthermore, sequential replacement of all wing feathers can take 3 to 10 months (63) when only the few longest primaries effectively determine wing length. Our data do not hold sufficient detail to filter out only individuals that were replacing critical feathers, but banders have typically not measured wing cord when these feathers were growing, leading to fewer wing measurements relative to mass. Barring directional shifts through time in age ratio, sex ratio, breeding, and molting, we control for the complexities above by standardizing the sampling period to dry season only. Such shifts would themselves represent a notable effect of climate change on Amazonian avifauna. However, filtering the entire dataset by categories we have only recently begun to understand could itself introduce systemic biases.

We categorized species into 12 foraging guilds and four vertical forest strata (table S6). Traits follow previously published work, which based assignments on behavioral observations and fecal samples throughout BDFFP sampling (9).

### Climate data

To test for correlations between climate and changes in body mass, wing length, and mass:wing ratio, and to test for long-term climate trends at our study site, we obtained temperature and precipitation estimates from the global EU Copernicus ERA5 climate reanalysis (<https://cds.climate.copernicus.eu>). These estimates, which are produced by combining physics-based climate models with historical data from weather stations and remote sensing, have a spatial resolution of 0.25° latitude × 0.25° longitude and a temporal resolution of 1 hour. Although reanalysis data for parts of Amazonia are affected by low number of weather stations, time trends in our models matched large-scale estimates from climate models for the region (45), and the last widespread drought was evident in our climate data (Fig. 1B). However, we caution that the quality of reanalysis data for the BDFFP will be likely lower than for regions with higher station density. We downloaded monthly averaged data, which provided the monthly means of (i) daily mean temperature and (ii) daily total precipitation, from ERA5 for 1966–1978 (64) and 1979–2019 (65). Temperature (“2 m temperature”) is the estimated air temperature at 2 m above ground level. Precipitation (“Total precipitation”) is the total precipitation estimated to have fallen during the time period. Our bird sampling locations fell within four raster cells (a 2 × 2 grid; Fig. 1A) of the ERA5 grid, and we thus averaged values for each month from these four grid cells to estimate an overall mean for our study area.

We used these monthly averaged daily values, based on average values for the four grid cells in which we captured birds, to produce estimates of mean temperature and total precipitation for the wet (December to May) and dry (June to November) seasons of each year. The wet season for year  $t$  was considered to start in December of year  $t - 1$ . We defined the seasons in this way to follow previous literature (9), a categorization based on broad annual precipitation patterns. We estimated mean temperature for each season and year by taking a weighted average of monthly mean values for the relevant

months, weighted by the number of days in each month. For total precipitation, we summed the product of each month’s mean daily total value and the number of days in that month. The dry and wet season estimates were then used as covariates in joint species distribution models (below). These models included covariates from several time lags, including the dry season in which a given individual was captured (“lag 0”; all captures occurred in the dry season), the wet season immediately preceding the dry season of capture (“lag 1”), and the dry season before the dry season of capture (“lag 2”).

### Statistical analysis

We quantified temporal trends in climate using generalized additive mixed models (GAMMs) implemented in R package *mgcv* (66, 67). First, to understand seasonal trends, we split climate data into dry and wet seasons as described above. We then used the *gamm()* function to specify GAMMs with autoregressive moving average (ARMA) error structures for each climate by season model. Covariates were modeled as the smooth of year with thin-plate basis ( $bs = tp$ ,  $k = 10$ ) and were fitted with restricted maximum likelihood and Gaussian distribution. To select the appropriate AR order, we set ARMA within year and selected the AR order on the basis of sequential likelihood ratio tests with the *anova()* function in R (68). The final model subsumed the structure of the last iteration that explained significant variation ( $\alpha \leq 0.05$ ).

We estimated change in body mass, wing length, and mass:wing ratio through time, and the effects of climatic covariates, using the Hierarchical Modelling of Species Communities (HMSC) R package (33, 69). This Bayesian joint species distribution model (70) differs from single species distribution models in that it uses a hierarchical structure to determine whether species’ responses to covariates are correlated with their traits and phylogenetic relationships. If so, these relationships among species with similar trait values or evolutionary histories can improve the quality of parameter estimates of individual species, especially for rare species for which data are relatively sparse (71). In total, we fitted 27 models (table S4), the specifics of which are detailed below. In addition to the multispecies models just described, these also include models for each response variable for the community as a whole, in which species are merged and treated as a random effect. All analyses were performed in R (68).

In our models, each individual bird was considered a sampling unit. Each row in our response variable input matrix thus represented an individual (denoted by band number), and each column represented 1 of our 77 species. For each row, the column corresponding to the correct species for that row had a numeric value (the response variable), and all other columns (species) in that row had a missing (NA) value. We fitted a similar set of models for each of three response variables: mass, wing length, and mass:wing ratio. All values of response were first centered on zero by subtracting the overall mean for the appropriate species from the measured value of a given individual (such that the centered overall mean for each species was zero). We then scaled these standardized values by dividing by 10 \* mean for each species, such that a value of 0.1 (–0.1) represented a measurement that was 1% higher (lower) than the mean value for that species. We assumed a normal error distribution for each response variable.

Together, this centering and scaling ensured that the default priors of the HMSC package were appropriate (69) and that the units of all measurements were consistent among species and biologically



meaningful (change as a % of body mass, wing length, or mass:wing), such that the hierarchical level in our models could best compare the responses of species (which differed in mean body size) on the basis of their trait values and phylogeny.

We fitted a set of identical models for predicting body mass, wing length, and mass:wing (table S4). These models included three different sets of predictor covariates: a year-only model, a year + temperature model, and a year + precipitation model (with year as a continuous covariate in each case). For the models that included temperature or precipitation climate covariates, three climate covariates were included: current dry season (lag 0), previous wet season (lag 1), and previous dry season (lag 2). For year-only models, raw (unstandardized) year values were used so that the units of the final coefficient estimates were intuitive. The HMSC package automatically scales all predictor covariates for model fitting, but then back-transforms parameter estimates to the original scale (69). For climate models, year and climate covariates were each scaled to have a mean of zero and an SD of one before input to HMSC so that all back-transformed predictor coefficients (“Beta” coefficients in HMSC terminology) would be at a similar scale, allowing us to easily compare their relative effects. The maximum variance inflation factor of any predictor covariate in any model was <2.01, indicating that multicollinearity was not a problem (72).

Our bird sampling took place across the entire dry season (June to November); to account for this temporal structure in our sampling, each model also included a random effect of month. Although residual variation at the broader scale is potentially of concern (i.e., unwanted factors affecting morphology in certain years), our covariates of interest materialize at the year scale—there is only one dry and wet season per year. Thus, any year effects that are not related to climate are confounded with annual-scale variation in morphology of interest. Nonetheless, we ran models similar to those in Figs. 1D and 4 but with the random effect of categorical year included (figs. S8 and S9). The conclusions persisted, but fewer species retained 95% CIs that did not overlap zero in models with climate covariates (fig. S9). Because extreme events (e.g., droughts) may affect morphology (fig. S10), and climate change likely increases the frequency of these events in Amazonia (73), we chose to not include random effect of year in our main analyses. We contend that the large number of sampling years ( $n = 26$ ) across the study interval helps to mediate any unwanted influence of arbitrary events that could manifest as time trend, especially of this taxonomically and ecologically diverse group of relatively long-lived endotherms in an environment that increasingly includes extremes (73).

Species with similar trait values, or a similar evolutionary history, often respond to their environment in similar ways (69). HMSC models include a hierarchical structure that estimates the strength of these effects in a community as a whole and uses these effects to inform the estimates for the responses of individual species to the environment. This is a particular benefit for rare species, for which fewer data points are available to estimate responses (71). We fitted a set of six models with foraging guild (categorical; 12 levels) as a trait, and an otherwise equivalent set of six models with foraging stratum (categorical; 4 levels) as a trait. These traits, guild and stratum, were not included in the same models because the two are highly correlated; foraging stratum is essentially a simplification of foraging guild, which is based on stratum as well as diet and foraging style. In HMSC terminology, the parameters that estimate the effects of traits on environmental responses are called “Gamma” parameters.

Each model also included a phylogeny, to test for phylogenetic correlation in species responses to the environment. Many traits are also phylogenetically structured, but the phylogenetic parameter in HMSC models tests only for phylogenetic correlation that is not explained by traits in the model. This means that phylogenetic signal is evidence of unmeasured underlying traits that are affecting responses (69). This parameter in the model ranges from 0 to 1, where 0 means that species responses are randomly distributed on the phylogeny and 1 indicates maximum phylogenetic structure. We used a phylogeny of all our species from Jetz *et al.* (74), downloaded from <https://birdtree.org>.

We fitted each Bayesian HMSC in R (75) using default diffuse prior distributions. We used six Markov Chain Monte Carlo (MCMC) chains to sample the posterior distributions of all parameters. Each chain was run for 100,000 iterations, with the first 50,000 discarded as burn-in. The remaining iterations were thinned by 50, producing 1000 samples per chain (6000 total). We evaluated effective sample size to assure adequate independence of samples and potential scale reduction factors (76) to assure model convergence. Model fitting was conducted with high performance computational resources provided by Louisiana State University ([www.hpc.lsu.edu](http://www.hpc.lsu.edu)).

We evaluated the explanatory power of each model for each species by examining  $R^2$  values, which were based on the correlation between model predictions for each sampling unit (i.e., individual bird) and the actual data. In addition, we examined the influence of each covariate using variance partitioning, which determines what percent of a model’s explanatory power can be attributed to each covariate and to any random effects. All variance partitioning values for each species were multiplied by the explanatory  $R^2$  value of that species to show amount of total variation in the response variable explained by each covariate.

Because of our scaling of the response variables before modeling, the raw Beta coefficients, showing each species’ responses to year, represented the change in body mass, wing length, or mass:wing per decade as a percentage of overall mean values for that species. This was reasonable for the purposes of our comparisons in the climate models, where we were interested in the relative strengths of responses to each covariate. For the year-only models, however, we wished to document the changes in morphological measurements relative to an appropriate baseline. To convert this raw estimate to percent of estimated 1980 mass, wing, and mass:wing (year zero as the first full year of sampling in our study), we multiplied each MCMC sample (from the appropriate coefficient’s distribution for each species) by a correction factor, which was calculated as the overall mean for a species divided by the median model estimate for 1980 for that species.

We next determined whether species with similar traits had similar responses to the environment and estimated overall mean change through time for mass, wing length, and mass:wing of each foraging guild and stratum as a whole. To determine the effects of traits on responses to the environment, we extracted Gamma parameters from each model, added them to the Gamma intercept to get the overall effect for each group, and summarized them by calculating quantiles. These Gamma parameters indicated the mean estimated response of species with a given (in this case) categorical trait level to a given environmental covariate (one Gamma parameter is estimated for each categorical trait level for each environmental covariate). We also used variance partitioning to estimate the proportion of variation in species responses to each covariate that was explained by traits.

To determine whether changes in mass, wing length, and mass:wing through time were phylogenetically correlated, we calculated “Moran’s  $I$ ” for Beta coefficient estimates for year from year-only models (with foraging guild as a trait) for each response variable using the phylo signal package (77) in R. Moran’s  $I$  is an estimate of autocorrelation in values along a phylogeny. We also calculated the correlation in Beta estimates as a function of phylogenetic distance and used nonparametric bootstrapping to produce confidence intervals (77). Last, we calculated a local Moran’s  $I$  value for each species, which is an estimate of how much that species’ location on the phylogeny helps to predict the value of its Beta coefficient.  $P$  values for each value of local Moran’s  $I$  were estimated using a nonparametric randomization test (77).

To determine whether morphological changes were associated with changes in abundance, we compared our results with species-specific trends from a continuous primary forest at the BDFFP [coefficients from Fig. 2A; (9)]. Because species are not independent and closely related species may show convergent patterns, we first needed to generate a phylogenetic hypothesis of all species in this study. To determine the most probable outcome, we relied on a maximum clade credibility tree built from 100 pseudo-posterior trees in the same phylogeny we used for our HMSC models (74), constrained by the Hackett backbone (78). We then fit linear models using phylogenetic generalized least-squares (PGLS) in the R package caper (79), which allowed the phylogenetic signal ( $\lambda$ ) in the data to be optimized by maximum likelihood. For all PGLS regressions (figs. S2 and S7), the null hypothesis (with associated  $P$  values) was slope equal to zero.

Our HMSC models explained on average 5.4 to 10.5% of the variation in body mass, 6.3 to 12.2% of the variation in wing length, and 9.9 to 15.0% of variation in mass:wing (table S4). Relatively low model fit was expected because we were modeling variation among years with year-level covariates and were not attempting to explain variation at the scale of individual birds, where variation was also substantial. Variance partitioning revealed that temperature explained more variation in mass on average in the climate models than did the year covariate, but year was more important than precipitation (fig. S11). For wing and mass:wing, year was more important in climate models than either temperature or precipitation (figs. S12 and S13).

Changes in mass, wing length, and mass:wing over time, and responses to climate covariates, were for the most part not correlated with species traits (figs. S1, S3, and S4). There was, however, a high degree of phylogenetic correlation in these responses in all models. Rates of morphological change in particular were phylogenetically correlated (fig. S14), with some regions of the phylogeny showing consistently high or low rates of change (figs. S15 and S16). For example, *Platyrinchus* spp. declined much more in body mass than did *Sclerurus* spp., whereas that was not the case for wing length. Species-specific predicted trends in mass, wing, and mass:wing from year-only models are shown in figs. S17, S18, and S19, respectively.

In addition to our main investigation using Bayesian HMSC models, we used LMMs. LMMs were used for two purposes: (i) to test for the effect of bird age on morphology and (ii) to conduct a parallel analysis of morphological change in the classical statistical framework to address possible concerns about attributes of Bayesian statistics or HMSC (e.g., influence of phylogeny and traits on model parameters). We implemented LMMs with the lmer() function in the R package lme4 (80). LMMs were similar in structure to associated HMSC models—we included the random effect of month and

species (tables S1 to S3). For LMMs of morphology by age, only random effect of species was included (table S5). We fit models using maximum likelihood where model comparison using AIC may be desirable (81), such as across metrics presented in tables S1 to S3. LMMs of morphology by age (table S5) and climate (fig. S5) were fit with restricted maximum likelihood. Climate covariates in fig. S5 were scaled to facilitate comparison of covariate effects across the three metrics. For LMM output with  $P$  values, parameter significance was assessed using the Satterthwaite method.

## SUPPLEMENTARY MATERIALS

Supplementary material for this article is available at <https://science.org/doi/10.1126/sciadv.abk1743>

## REFERENCES AND NOTES

1. T. P. Hughes, M. L. Barnes, D. R. Bellwood, J. E. Cinner, G. S. Cumming, J. B. C. Jackson, J. Kleypas, I. A. van de Leemput, J. M. Lough, T. H. Morrison, S. R. Palumbi, E. H. van Nes, M. Scheffer, Coral reefs in the Anthropocene. *Nature* **546**, 82–90 (2017).
2. C. D. Allen, D. D. Breshears, N. G. McDowell, On underestimation of global vulnerability to tree mortality and forest die-off from hotter drought in the Anthropocene. *Ecosphere* **6**, 129 (2015).
3. D. Jablonski, K. Roy, J. W. Valentine, Out of the tropics: Evolutionary dynamics of the latitudinal diversity gradient. *Science* **314**, 102–106 (2006).
4. J. Rolland, F. L. Condamine, F. Jiguet, H. Morlon, Faster speciation and reduced extinction in the tropics contribute to the mammalian latitudinal diversity gradient. *PLOS Biol.* **12**, e1001775 (2014).
5. M. J. P. Sullivan, S. L. Lewis, K. Affum-Baffoe, C. Castilho, F. Costa, A. C. Sanchez, C. E. N. Ewango, W. Hubau, B. Marimon, A. Monteagudo-Mendoza, L. Qie, B. Sonké, R. V. Martinez, T. R. Baker, R. J. W. Brienen, T. R. Feldpausch, D. Galbraith, M. Gloor, Y. Malhi, S.-I. Aiba, M. N. Alexiades, E. C. Almeida, E. A. de Oliveira, E. Á. Dávila, P. A. Loayza, A. Andrade, S. A. Vieira, L. E. O. C. Aragão, A. Araujo-Murakami, E. J. M. M. Arets, L. Arroyo, P. Ashton, G. Aymard, C. F. B. Baccaro, L. F. Banin, C. Baraloto, P. B. Camargo, J. Barlow, J. Barroso, J.-F. Bastin, S. A. Batterman, H. Beeckman, S. K. Begne, A. C. Bennett, E. Berenguer, N. Berry, L. Blanc, P. Boeckx, J. Bogaert, D. Bonal, F. Bongers, M. Bradford, F. D. Brearley, T. Brncic, F. Brown, B. Burban, J. L. Camargo, W. Castro, C. Céron, S. C. Ribeiro, V. C. Moscoso, J. Chave, E. Chezeaux, C. J. Clark, F. C. de Souza, M. Collins, J. A. Comiskey, F. C. Valverde, M. C. Medina, L. da Costa, M. Dančák, G. C. Dargie, S. Davies, N. D. Cardozo, T. de Haulleville, M. B. de Medeiros, J. Del Aguila Pasquel, G. Derroire, A. D. Fiore, J.-L. Doucet, A. Dourdain, V. Droissart, L. F. Duque, R. Ekoungoulou, F. Elias, T. Erwin, A. Esquivel-Muelbert, S. Fauset, J. Ferreira, G. F. Llampazo, E. Foli, A. Ford, M. Gilpin, J. S. Hall, K. C. Hamer, A. C. Hamilton, D. J. Harris, T. B. Hart, R. Hédli, B. Herault, R. Herrera, N. Higuchi, A. Hladik, E. H. Coronado, I. Huamantupa-Chuquimaco, W. H. Huasco, K. J. Jeffery, E. Jimenez-Rojas, M. Kalamandeen, M. N. K. Djuikouo, E. Kearsley, R. K. Umetsu, L. K. Kho, T. Killeen, K. Kitayama, B. Klitgaard, A. Koch, N. Labrière, W. Laurance, S. Laurance, M. E. Leal, A. Levesley, A. J. N. Lima, J. Lisings, A. P. Lopes, G. Lopez-Gonzalez, T. Lovejoy, J. C. Lovett, R. Lowe, W. E. Magnusson, J. Malumbres-Olarte, Á. G. Manzatto, B. H. Marimon, A. R. Marshall, T. Marthews, S. M. de Almeida Reis, C. Maycock, K. Melgaço, C. Mendoza, F. Metali, V. Mihindou, W. Milliken, E. T. A. Mitchard, P. S. Morandi, H. L. Mossman, L. Nagy, H. Nascimento, D. Neill, R. Nilus, P. N. Vargas, W. Palacios, N. P. Camacho, J. Peacock, C. Pendry, M. C. P. Mora, G. C. Pickavance, J. Pipoly, N. Pitman, M. Playfair, L. Poorter, J. R. Poulsen, A. D. Poulsen, R. Preziosi, A. Prieto, R. B. Primack, H. Ramírez-Angulo, J. Reitsma, M. Réjou-Méchain, Z. R. Correa, T. R. de Sousa, L. R. Bayona, A. Roopsind, A. Rudas, E. Rutishauser, K. A. Salim, R. P. Salomão, J. Schiatti, D. Sheil, R. C. Silva, J. S. Espejo, C. S. Valeria, M. Silveira, M. Simo-Droissart, M. F. Simon, J. Singh, Y. C. S. Shareva, C. Stahl, J. Stropp, R. Sukri, T. Sunderland, M. Svátek, M. D. Swaine, V. Swamy, H. Taedoumg, J. Talbot, J. Taplin, D. Taylor, H. ter Steege, J. Terborgh, R. Thomas, S. C. Thomas, A. Torres-Lezama, P. Umunay, L. V. Gamarra, G. van der Heijden, P. van der Hout, P. van der Meer, M. van Nieuwstadt, H. Verbeeck, R. Verminnen, A. Vicentini, I. C. G. Vieira, E. V. Torre, J. Vleminckx, V. Vos, O. Wang, L. J. T. White, S. Willcock, J. T. Woods, V. Wortel, K. Young, R. Zagt, L. Zedler, P. A. Zuidema, J. A. Zwarts, O. L. Phillips, Long-term thermal sensitivity of Earth’s tropical forests. *Science* **368**, 869–874 (2020).
6. A. Esquivel-Muelbert, T. R. Baker, K. G. Dexter, S. L. Lewis, R. J. W. Brienen, T. R. Feldpausch, J. Lloyd, A. Monteagudo-Mendoza, L. Arroyo, E. Álvarez-Dávila, N. Higuchi, B. S. Marimon, B. H. Marimon-Junior, M. Silveira, E. Vilanova, E. Gloor, Y. Malhi, J. Chave, J. Barlow, D. Bonal, N. D. Cardozo, T. Erwin, S. Fauset, B. Hérault, S. Laurance, L. Poorter, L. Qie, C. Stahl, M. J. P. Sullivan, H. ter Steege, V. A. Vos, P. A. Zuidema, E. Almeida, E. A. de Oliveira, A. Andrade, S. A. Vieira, L. Aragão, A. Araujo-Murakami, E. Arets,

- G. A. Aymard, C. Baraloto, P. B. Camargo, J. G. Barroso, F. Bongers, R. Boot, J. L. Camargo, W. Castro, V. C. Moscoso, J. Comiskey, F. C. Valverde, A. C. L. da Costa, J. del Aguila Pasquel, A. D. Fiore, L. F. Duque, F. Elias, J. Engel, G. F. Llampazo, D. Galbraith, R. H. Fernández, E. H. Coronado, W. Hubau, E. Jimenez-Rojas, A. J. N. Lima, R. K. Umetsu, W. Laurance, G. Lopez-Gonzalez, T. Lovejoy, O. A. M. Cruz, P. S. Morandi, D. Neill, P. N. Vargas, N. C. P. Camacho, A. P. Gutierrez, G. Pardo, J. Peacock, M. Peña-Claros, M. C. Peñuela-Mora, P. Petronelli, G. C. Pickavance, N. Pitman, A. Prieto, C. Quesada, H. Ramirez-Angulo, M. Réjou-Méchain, Z. R. Correa, A. Roopsind, A. Rudas, R. Salomão, N. Silva, J. S. Espejo, J. Singh, J. Stropp, J. Terborgh, R. Thomas, M. Toledo, A. Torres-Lezama, L. V. Gamarra, P. J. van de Meer, G. van der Heijden, P. van der Hout, R. V. Martinez, C. Vela, I. C. G. Vieira, O. L. Phillips, Compositional response of Amazon forests to climate change. *Glob. Chang. Biol.* **25**, 39–56 (2019).
7. M. L. Morrison, Bird populations as indicators of environmental change, in *Current Ornithology: Volume 3*, R. F. Johnston, Ed. (Current Ornithology, Springer, 1986), pp. 429–451.
8. M. G. Harvey, G. A. Bravo, S. Claramunt, A. M. Cuervo, G. E. Derryberry, J. Battilana, G. F. Seeholzer, J. S. McKay, B. C. O'Meara, B. C. Faircloth, S. V. Edwards, J. Pérez-Emán, R. G. Moyle, F. H. Sheldon, A. Aleixo, B. T. Smith, R. T. Chesser, L. F. Silveira, J. Cracraft, R. T. Brumfield, E. P. Derryberry, The evolution of a tropical biodiversity hotspot. *Science* **370**, 1343–1348 (2020).
9. P. C. Stouffer, V. Jirinec, C. L. Rutt, R. O. Bierregaard Jr., A. Hernández-Palma, E. I. Johnson, S. R. Midway, L. L. Powell, J. D. Wolfe, T. E. Lovejoy, Long-term change in the avifauna of undisturbed Amazonian rainforest: Ground-foraging birds disappear and the baseline shifts. *Ecol. Lett.* **24**, 186–195 (2021).
10. J. G. Blake, B. A. Loiselle, Enigmatic declines in bird numbers in lowland forest of eastern Ecuador may be a consequence of climate change. *PeerJ* **3**, e1177 (2015).
11. C. T. Almeida, J. F. Oliveira-Júnior, R. C. Delgado, P. Cubo, M. C. Ramos, Spatiotemporal rainfall and temperature trends throughout the Brazilian Legal Amazon, 1973–2013. *Int. J. Climatol.* **37**, 2013–2026 (2017).
12. R. B. Huey, M. R. Kearney, A. Krockenberger, J. A. M. Holtum, M. Jess, S. E. Williams, Predicting organismal vulnerability to climate warming: Roles of behaviour, physiology and adaptation. *Philos. Trans. R. Soc. B Biol. Sci.* **367**, 1665–1679 (2012).
13. K. S. Sheldon, R. B. Huey, M. Kaspari, N. J. Sanders, Fifty years of mountain passes: A perspective on Dan Janzen's classic article. *Am. Nat.* **191**, 553–565 (2018).
14. J. L. Gardner, A. Peters, M. R. Kearney, L. Joseph, R. Heinsohn, Declining body size: A third universal response to warming? *Trends Ecol. Evol.* **26**, 285–291 (2011).
15. C. Bergmann, Über die verhältnisse der wärmeökonomie der thiere zu ihrer gröÙe. *Göttinger Studien* **3**, 595–708 (1847).
16. E. Mayr, Geographical character gradients and climatic adaptation. *Evolution* **10**, 105–108 (1956).
17. K. G. Ashton, Patterns of within-species body size variation of birds: Strong evidence for Bergmann's rule. *Glob. Ecol. Biogeogr.* **11**, 505–523 (2002).
18. C. Watt, S. Mitchell, V. Salewski, Bergmann's rule; a concept cluster? *Oikos* **119**, 89–100 (2010).
19. C. Parmesan, G. Yohe, A globally coherent fingerprint of climate change impacts across natural systems. *Nature* **421**, 37–42 (2003).
20. J. M. Durant, D. Ø. Hjernann, G. Ottersen, N. C. Stenseth, Climate and the match or mismatch between predator requirements and resource availability. *Climate Res.* **33**, 271–283 (2007).
21. M. Daufresne, K. Lengfellner, U. Sommer, Global warming benefits the small in aquatic ecosystems. *Proc. Natl. Acad. Sci. U.S.A.* **106**, 12788–12793 (2009).
22. C. Teplitsky, V. Millien, Climate warming and Bergmann's rule through time: Is there any evidence? *Evol. Appl.* **7**, 156–168 (2014).
23. S. Messina, D. Costantini, S. Tomassi, C. C. P. Cosset, S. Benedick, M. Eens, D. P. Edwards, Selective logging reduces body size in omnivorous and frugivorous tropical forest birds. *Biol. Conserv.* **256**, 109036 (2021).
24. E. C. Ellis, K. K. Goldewijk, S. Siebert, D. Lightman, N. Ramankutty, Anthropogenic transformation of the biomes, 1700 to 2000. *Glob. Ecol. Biogeogr.* **19**, 589–606 (2010).
25. L. V. Alexander, X. Zhang, T. C. Peterson, J. Caesar, B. Gleason, A. M. G. K. Tank, M. Haylock, D. Collins, B. Trewin, F. Rahimzadeh, A. Tagipour, K. R. Kumar, J. Revadekar, G. Griffiths, L. Vincent, D. B. Stephenson, J. Burn, E. Aguilar, M. Brunet, M. Taylor, M. New, P. Zhai, M. Rusticucci, J. L. Vazquez-Aguirre, Global observed changes in daily climate extremes of temperature and precipitation. *J. Geophys. Res. Atmos.* **111**, D05109 (2006).
26. B. C. Weeks, D. E. Willard, M. Zimova, A. A. Ellis, M. L. Witynski, M. Hennen, B. M. Winger, Shared morphological consequences of global warming in North American migratory birds. *Ecol. Lett.* **23**, 316–325 (2020).
27. M. C. Urban, Accelerating extinction risk from climate change. *Science* **348**, 571–573 (2015).
28. F. E. Hayes, J.-A. N. Sewlal, The Amazon River as a dispersal barrier to passerine birds: Effects of river width, habitat and taxonomy. *J. Biogeogr.* **31**, 1809–1818 (2004).
29. S. J. Wright, H. C. Muller-Landau, J. Schipper, The future of tropical species on a warmer planet. *Conserv. Biol.* **23**, 1418–1426 (2009).
30. R. A. Bay, R. J. Harrigan, V. L. Underwood, H. L. Gibbs, T. B. Smith, K. Ruegg, Genomic signals of selection predict climate-driven population declines in a migratory bird. *Science* **359**, 83–86 (2018).
31. C. L. Rutt, V. Jirinec, M. Cohn-Haft, W. F. Laurance, P. C. Stouffer, Avian ecological succession in the Amazon: A long-term case study following experimental deforestation. *Ecol. Evol.* **9**, 13850–13861 (2019).
32. M. K. Labocha, J. P. Hayes, Morphometric indices of body condition in birds: A review. *J. Ornithol.* **153**, 1–22 (2012).
33. O. Ovaskainen, G. Tikhonov, A. Norberg, F. G. Blanchet, L. Duan, D. Dunson, T. Roslin, N. Abrego, How to make more out of community data? A conceptual framework and its implementation as models and software. *Ecol. Lett.* **20**, 561–576 (2017).
34. E. A. Riddell, K. J. Iknayan, L. Hargrove, S. Tremor, J. L. Patton, R. Ramirez, B. O. Wolf, S. R. Beissinger, Exposure to climate change drives stability or collapse of desert mammal and bird communities. *Science* **371**, 633–636 (2021).
35. D. H. Janzen, Why mountain passes are higher in the tropics. *Am. Nat.* **101**, 233–249 (1967).
36. F. C. James, Geographic size variation in birds and its relationship to climate. *Ecology* **51**, 365–390 (1970).
37. J. Van Buskirk, R. S. Mulvihill, R. C. Leberman, Declining body sizes in North American birds associated with climate change. *Oikos* **119**, 1047–1055 (2010).
38. J. A. Allen, The influence of physical conditions in the genesis of species. *Radic. Rev.* **1**, 108–140 (1877).
39. J. L. Gardner, T. Amano, P. R. Y. Backwell, K. Ikin, W. J. Sutherland, A. Peters, Temporal patterns of avian body size reflect linear size responses to broadscale environmental change over the last 50 years. *J. Avian Biol.* **45**, 529–535 (2014).
40. M. S. Bowlin, M. Wikelski, Pointed wings, low wingloading and calm air reduce migratory flight costs in songbirds. *PLOS ONE* **3**, e2154 (2008).
41. R. P. Moore, W. D. Robinson, I. J. Lovette, T. R. Robinson, Experimental evidence for extreme dispersal limitation in tropical forest birds. *Ecol. Lett.* **11**, 960–968 (2008).
42. S. G. W. Laurance, P. C. Stouffer, W. F. Laurance, Effects of road clearings on movement patterns of understory rainforest birds in central Amazonia. *Conserv. Biol.* **18**, 1099–1109 (2004).
43. W. A. Boyle, E. H. Shogren, J. D. Brawn, Hygric niches for tropical endotherms. *Trends Ecol. Evol.* **35**, 938–952 (2020).
44. X. Feng, A. Porporato, I. Rodriguez-Iturbe, Changes in rainfall seasonality in the tropics. *Nat. Clim. Change* **3**, 811–815 (2013).
45. R. K. Pachauri, M. R. Allen, V. R. Barros, J. Broome, W. Cramer, R. Christ, J. A. Church, L. Clarke, Q. Dahe, P. Dasgupta, *Climate change 2014: Synthesis report. Contribution of Working Groups I, II and III to the fifth assessment report of the Intergovernmental Panel on Climate Change* (IPCC, 2014).
46. T. Alerstam, M. Rosén, J. Bäckman, P. G. P. Ericson, O. Hellgren, Flight speeds among bird species: Allometric and phylogenetic effects. *PLOS Biol.* **5**, e197 (2007).
47. A. A. Hoffmann, C. M. Sgrò, Climate change and evolutionary adaptation. *Nature* **470**, 479–485 (2011).
48. P. Gienapp, C. Teplitsky, J. S. Alho, J. A. Mills, J. Merilä, Climate change and evolution: Disentangling environmental and genetic responses. *Mol. Ecol.* **17**, 167–178 (2008).
49. D. H. Ho, W. W. Burggren, Epigenetics and transgenerational transfer: A physiological perspective. *J. Exp. Biol.* **213**, 3–16 (2010).
50. T. D. Price, P. R. Grant, H. L. Gibbs, P. T. Boag, Recurrent patterns of natural selection in a population of Darwin's finches. *Nature* **309**, 787–789 (1984).
51. N. Dubos, I. Le Viol, A. Robert, C. Teplitsky, M. Ghislin, O. Dehorter, R. Julliard, P. Y. Henry, Disentangling the effects of spring anomalies in climate and net primary production on body size of temperate songbirds. *Ecography* **41**, 1319–1330 (2018).
52. E. I. Johnson, J. D. Wolfe, *Molt in Neotropical Birds: Life History and Aging Criteria* (CRC Press, ed. 1, 2017).
53. B. A. Walther, Vertical stratification and use of vegetation and light habitats by Neotropical forest birds. *J. Ornithol.* **143**, 64–81 (2002).
54. B. R. Scheffers, B. L. Phillips, W. F. Laurance, N. S. Sodhi, A. Diesmos, S. E. Williams, Increasing arboreality with altitude: A novel biogeographic dimension. *Proc. R. Soc. B Biol. Sci.* **280**, 20131581 (2013).
55. M. H. C. Neate-Clegg, T. R. Stanley, Ç. H. Şekericioğlu, W. D. Newmark, Temperature-associated decreases in demographic rates of Afrotropical bird species over 30 years. *Glob. Chang. Biol.* **27**, 2254–2268 (2021).
56. L. L. Powell, N. J. Cordeiro, J. A. Stratford, Ecology and conservation of avian insectivores of the rainforest understory: A pantropical perspective. *Biol. Conserv.* **188**, 1–10 (2015).



57. K. V. Rosenberg, A. M. Dokter, P. J. Blancher, J. R. Sauer, A. C. Smith, P. A. Smith, J. C. Stanton, A. Panjabi, L. Helft, M. Parr, P. P. Marra, Decline of the North American avifauna. *Science* **366**, 120–124 (2019).
58. P. C. Stouffer, Birds in fragmented Amazonian rainforest: Lessons from 40 years at the Biological Dynamics of Forest Fragments Project. *Condor* **122**, duaa005 (2020).
59. V. Jirinec, P. F. Rodrigues, B. Amaral, Adjustable leg harness for attaching tags to small and medium-sized birds. *J. Field Ornithol.* **92**, 77–87 (2021).
60. E. Lehtikoinen, Seasonality of the daily weight cycle in wintering passerines and its consequences. *Ornis Scandinavica*. **18**, 216–226 (1987).
61. M. Moiron, K. J. Mathot, N. J. Dingemans, To eat and not be eaten: Diurnal mass gain and foraging strategies in wintering great tits. *Proc. R. Soc. B Biol. Sci.* **285**, 20172868 (2018).
62. P. C. Stouffer, E. I. Johnson, R. O. Bierregaard, Breeding seasonality in central Amazonian rainforest birds. *Auk* **130**, 529–540 (2013).
63. E. I. Johnson, P. C. Stouffer, R. O. Bierregaard Jr., The phenology of molting, breeding and their overlap in central Amazonian birds. *J. Avian Biol.* **43**, 141–154 (2012).
64. B. Bell, H. Hersbach, P. Berrisford, P. Dahlgren, A. Horányi, J. Muñoz Sabater, J. Nicolas, R. Radu, D. Schepers, A. Simmons, C. Soci, J.-N. Thépaut, ERA5 monthly averaged data on single levels from 1950 to 1978 (preliminary version), in *Copernicus Climate Change Service (C3S) Climate Data Store (CDS)* (2020); <https://cds.climate.copernicus.eu/cdsapp#!/dataset/reanalysis-era5-single-levels-monthly-means-preliminary-back-extension>.
65. H. Hersbach, B. Bell, P. Berrisford, G. Biavati, A. Horányi, J. Muñoz Sabater, J. Nicolas, C. Peubey, R. Radu, I. Rozum, D. Schepers, A. Simmons, C. Soci, D. Dee, J.-N. Thépaut, ERA5 monthly averaged data on single levels from 1979 to present, in *ERA5 monthly averaged data on single levels from 1979 to present*. *Copernicus Climate Change Service (C3S) Climate Data Store (CDS)* (2019); <https://doi.org/10.24381/cds.f17050d7>.
66. S. Wood, *Generalized Additive Models: An Introduction with R* (Chapman and Hall/CRC, 2017).
67. S. Wood, mgcv: Mixed GAM computation vehicle with automatic smoothness estimation (2020); <https://CRAN.R-project.org/package=mgcv>.
68. R Core Team, R: A language and environment for statistical computing (R Foundation for Statistical Computing, Vienna, Austria, 2020); [www.R-project.org](http://www.R-project.org).
69. O. Ovaskainen, N. Abrego, *Joint Species Distribution Modelling: With Applications in R* (Cambridge Univ. Press, 2020).
70. D. I. Warton, F. G. Blanchet, R. B. O'Hara, O. Ovaskainen, S. Taskinen, S. C. Walker, F. K. C. Hui, So many variables: Joint modeling in community ecology. *Trends Ecol. Evol.* **30**, 766–779 (2015).
71. N. Abrego, A. Norberg, O. Ovaskainen, Measuring and predicting the influence of traits on the assembly processes of wood-inhabiting fungi. *J. Ecol.* **105**, 1070–1081 (2017).
72. B. Naimi, N. A. S. Hamm, T. A. Groen, A. K. Skidmore, A. G. Toxopeus, Where is positional uncertainty a problem for species distribution modelling? *Ecography* **37**, 191–203 (2014).
73. T. R. Feldpausch, O. L. Phillips, R. J. W. Brienen, E. Gloor, J. Lloyd, G. Lopez-Gonzalez, A. Monteagudo-Mendoza, Y. Malhi, A. Alarcón, E. Á. Dávila, P. Alvarez-Loayza, A. Andrade, L. E. O. C. Aragao, L. Arroyo, G. A. Aymard, C. T. R. Baker, C. Baraloto, J. Barroso, D. Bonal, W. Castro, V. Chama, J. Chave, T. F. Domingues, S. Fauset, N. Groot, E. H. Coronado, S. Laurance, W. F. Laurance, S. L. Lewis, J. C. Licona, B. S. Marimon, B. H. Marimon-Junior, C. M. Bautista, D. A. Neill, E. A. Oliveira, C. O. dos Santos, N. C. P. Camacho, G. Pardo-Molina, A. Prieto, C. A. Quesada, F. Ramírez, H. Ramírez-Angulo, M. Réjou-Méchain, A. Rudas, G. Saiz, R. P. Salomão, J. E. Silva-Espejo, M. Silveira, H. ter Steege, J. Stropp, J. Terborgh, R. Thomas-Caesar, G. M. F. van der Heijden, R. V. Martinez, E. Vilanova, V. A. Vos, Amazon forest response to repeated droughts. *Global Biogeochem. Cycles* **30**, 964–982 (2016).
74. W. Jetz, G. H. Thomas, J. B. Joy, K. Hartmann, A. O. Mooers, The global diversity of birds in space and time. *Nature* **491**, 444–448 (2012).
75. G. Tikhonov, Ø. H. Opedal, N. Abrego, A. Lehtikoinen, M. M. J. de Jonge, J. Oksanen, O. Ovaskainen, Joint species distribution modelling with the R-package H<sub>MSC</sub>. *Methods Ecol. Evol.* **11**, 442–447 (2020).
76. S. P. Brooks, A. Gelman, General methods for monitoring convergence of iterative simulations. *J. Comput. Graph. Stat.* **7**, 434–455 (1998).
77. F. Keck, F. Rimet, A. Bouchez, A. Franc, phylosignal: An R package to measure, test, and explore the phylogenetic signal. *Ecol. Evol.* **6**, 2774–2780 (2016).
78. S. J. Hackett, R. T. Kimball, S. Reddy, R. C. K. Bowie, E. L. Braun, M. J. Braun, J. L. Chojnowski, W. A. Cox, K.-L. Han, J. Harshman, C. J. Huddleston, B. D. Marks, K. J. Miglia, W. S. Moore, F. H. Sheldon, D. W. Steadman, C. C. Witt, T. Yuri, A phylogenomic study of birds reveals their evolutionary history. *Science* **320**, 1763–1768 (2008).
79. D. Orme, R. Freckleton, G. Thomas, T. Petzoldt, S. Fritz, N. Isaac, W. Pearse, caper: Comparative analyses of phylogenetics and evolution in R (2018); <https://CRAN.R-project.org/package=caper>.
80. D. Bates, M. Maechler, B. Bolker, S. Walker, R. H. B. Christensen, H. Singmann, B. Dai, F. Scheipl, G. Grothendieck, P. Green, J. Fox, lme4: Linear mixed-effects models using “Eigen” and S4 (2020); <https://CRAN.R-project.org/package=lme4>.
81. A. Zuur, E. N. Ieno, N. Walker, A. A. Saveliev, G. M. Smith, *Mixed Effects Models and Extensions in Ecology with R* (Statistics for Biology and Health, Springer-Verlag, 2009).
82. J. A. Marengo, C. A. Nobre, J. Tomasella, M. D. Oyama, G. S. de Oliveira, R. de Oliveira, H. Camargo, L. M. Alves, I. F. Brown, The drought of Amazonia in 2005. *J. Climate* **21**, 495–516 (2008).
83. S. L. Lewis, P. M. Brando, O. L. Phillips, G. M. F. van der Heijden, D. Nepstad, The 2010 Amazon drought. *Science* **331**, 554–554 (2011).
84. A. Erfanian, G. Wang, L. Fomenko, Unprecedented drought over tropical South America in 2016: Significantly under-predicted by tropical SST. *Sci. Rep.* **7**, 5811 (2017).
85. J. A. Stratford, W. D. Robinson, Gulliver travels to the fragmented tropics: Geographic variation in mechanisms of avian extinction. *Front. Ecol. Environ.* **3**, 85–92 (2005).

**Acknowledgments:** We are indebted to all those who collected data over the years, with special thanks to *mateiros* J. Lopes and O. Pereira, and to ornithologists L. Figueira, P. Martins, and I. Coriolano, from the UFRGS Population Biology Laboratory. K. Mokross drafted forest artwork in Fig. 2. Bird illustrations provided by Lynx Edicions, used with permission. This is publication no. 822 of the BDFPP Technical Series and no. 60 of the Amazonian Ornithology Technical Series of the INPA Collections Program. The manuscript was approved by the Director of the Louisiana State University Agricultural Center as manuscript number 2021-241-36609. **Funding:** This work was supported by U.S. National Science Foundation LTREB grants 0545491 and 1257340 (P.C.S.), U.S. Department of Agriculture McIntire Stennis project nos. 94098 and 94327 (P.C.S.), World Wildlife Fund-U.S. (T.E.L. and R.O.B.), MacArthur Foundation (T.E.L. and R.O.B.), Andrew W. Mellon Foundation (T.E.L. and R.O.B.), U.S. Agency for International Development (T.E.L. and R.O.B.), U.S. National Aeronautics and Space Administration (T.E.L. and R.O.B.), Brazil's Ministry for Science and Technology (T.E.L. and R.O.B.), Smithsonian Tropical Research Institute (V.J.), Neotropical Bird Club (V.J.), American Philosophical Society (V.J.), American Ornithological Society (V.J.), Animal Behavior Society (V.J.), and Wilson Ornithological Society (V.J.). L.L.P. was supported via the European Union's Horizon 2020 research and innovation programme under grant agreement no. 854248. **Author contributions:** B.R.A. through J.D.W. are ranked alphabetically. Conceptualization: V.J., P.C.S., and T.E.L. Methodology: V.J., R.C.B., P.C.S., R.O.B., and T.E.L. Formal analysis: R.C.B., V.J., and C.L.R. Validation: R.C.B. Data curation: P.C.S. and V.J. Writing—original draft: V.J. and R.C.B. Writing—review and editing: all authors. Investigation: all authors. Visualization: V.J. and R.C.B. Supervision: P.C.S., T.E.L., and R.O.B. Project administration: P.C.S., T.E.L., and R.O.B. Funding acquisition: P.C.S., T.E.L., R.O.B., and V.J. **Competing interests:** The authors declare that they have no competing interests. **Data and materials availability:** All data needed to evaluate the conclusions in the paper are present in the paper and/or the Supplementary Materials. Morphometric and climate data used for analysis are archived and available on Dryad at <https://doi.org/10.5061/dryad.fqz612j>.

Submitted 25 June 2021  
 Accepted 16 September 2021  
 Published 12 November 2021  
 10.1126/sciadv.abk1743



## Morphological consequences of climate change for resident birds in intact Amazonian rainforest

Vitek JirinecRyan C. BurnerBruna R. AmaralRichard O. Bierregaard Jr.Gilberto Fernández-ArellanoAngélica Hernández-PalmaErik I. JohnsonThomas E. LovejoyLuke L. PowellCameron L. RuttJared D. WolfePhilip C. Stouffer

*Sci. Adv.*, 7 (46), eabk1743.

### View the article online

<https://www.science.org/doi/10.1126/sciadv.abk1743>

### Permissions

<https://www.science.org/help/reprints-and-permissions>

Use of think article is subject to the [Terms of service](#)

---

*Science Advances* (ISSN ) is published by the American Association for the Advancement of Science. 1200 New York Avenue NW, Washington, DC 20005. The title *Science Advances* is a registered trademark of AAAS. Copyright © 2021 The Authors, some rights reserved; exclusive licensee American Association for the Advancement of Science. No claim to original U.S. Government Works. Distributed under a Creative Commons Attribution NonCommercial License 4.0 (CC BY-NC).

Supplementary Materials for  
**Morphological consequences of climate change for resident birds in intact  
Amazonian rainforest**

Vitek Jirinec\*, Ryan C. Burner, Bruna R. Amaral, Richard O. Bierregaard Jr.,  
Gilberto Fernández-Arellano, Angélica Hernández-Palma, Erik I. Johnson, Thomas E. Lovejoy,  
Luke L. Powell, Cameron L. Rutt, Jared D. Wolfe, Philip C Stouffer

\*Corresponding author. Email: [vjirin1@lsu.edu](mailto:vjirin1@lsu.edu)

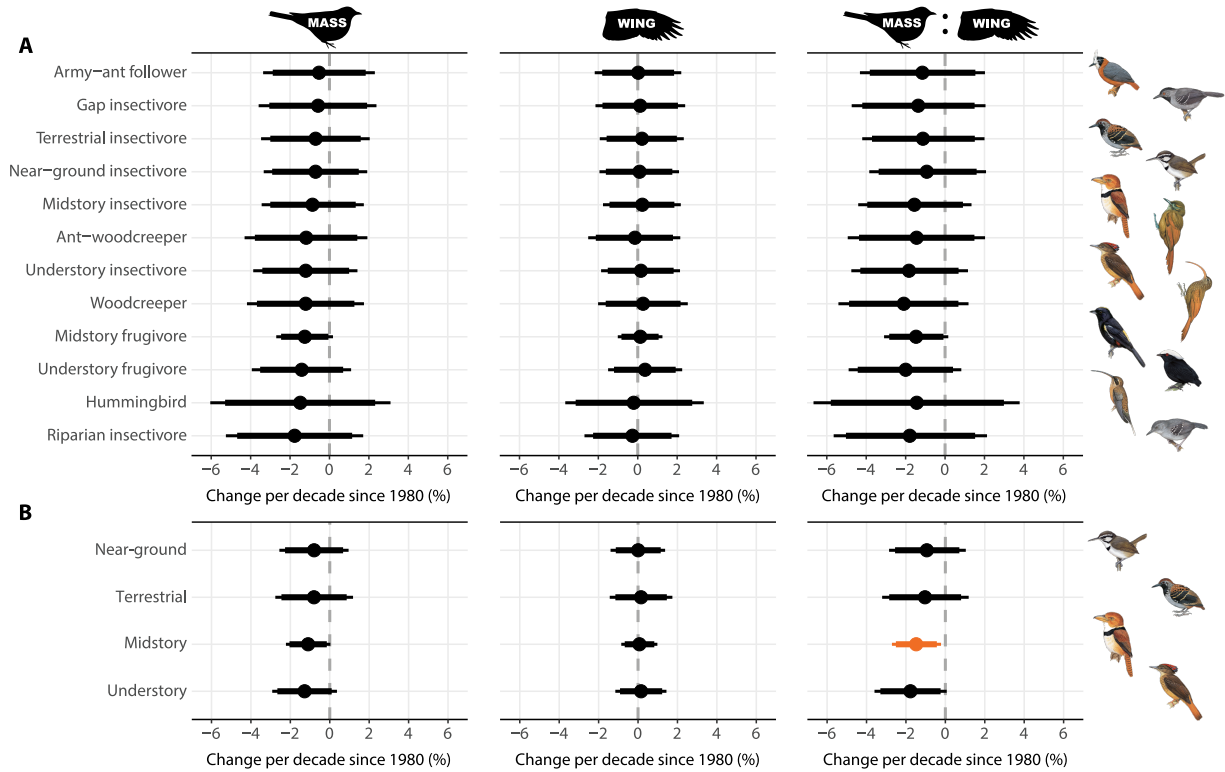
Published 12 November 2021, *Sci. Adv.* **7**, eabk1743 (2021)

DOI: [10.1126/sciadv.abk1743](https://doi.org/10.1126/sciadv.abk1743)

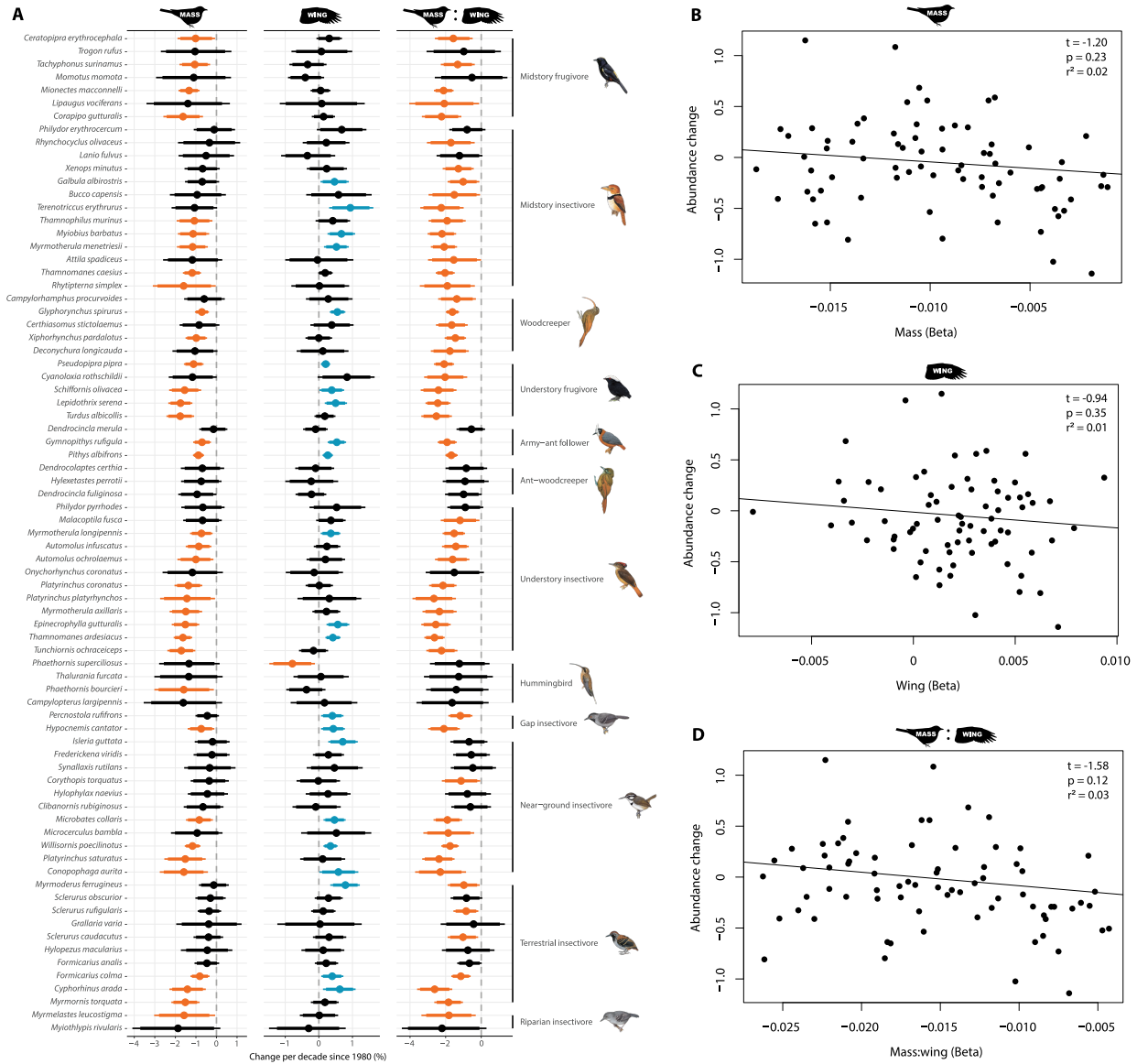
**This PDF file includes:**

Figs. S1 to S19

Tables S1 to S6

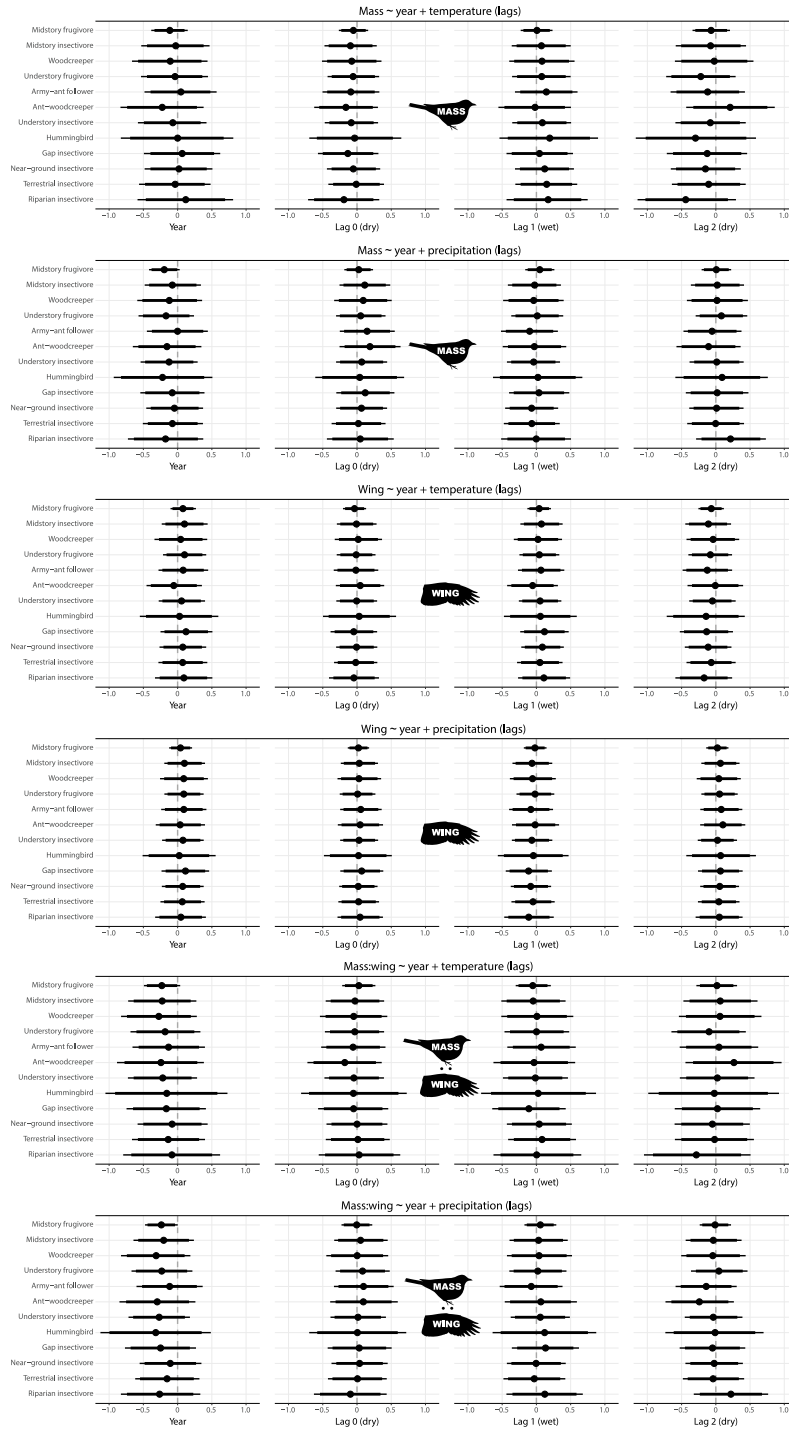


**Fig. S1. Bird morphology time trends by ecological traits. (A) Foraging guilds. (B) Vertical forest stratum.** In both panels, points show the overall estimate of change through time for a given group of species, from the second level (Gamma parameters) of a hierarchical model of individual species trends. Lines represent 90% and 95% credible intervals. (A) shows Gamma parameters for model depicted in Fig. 1D whereas (B) shows output from an identical model with stratum (rather than guild) as the species trait. Results correspond to models 1, 7, 13, 4, 10, and 16 (table S4).

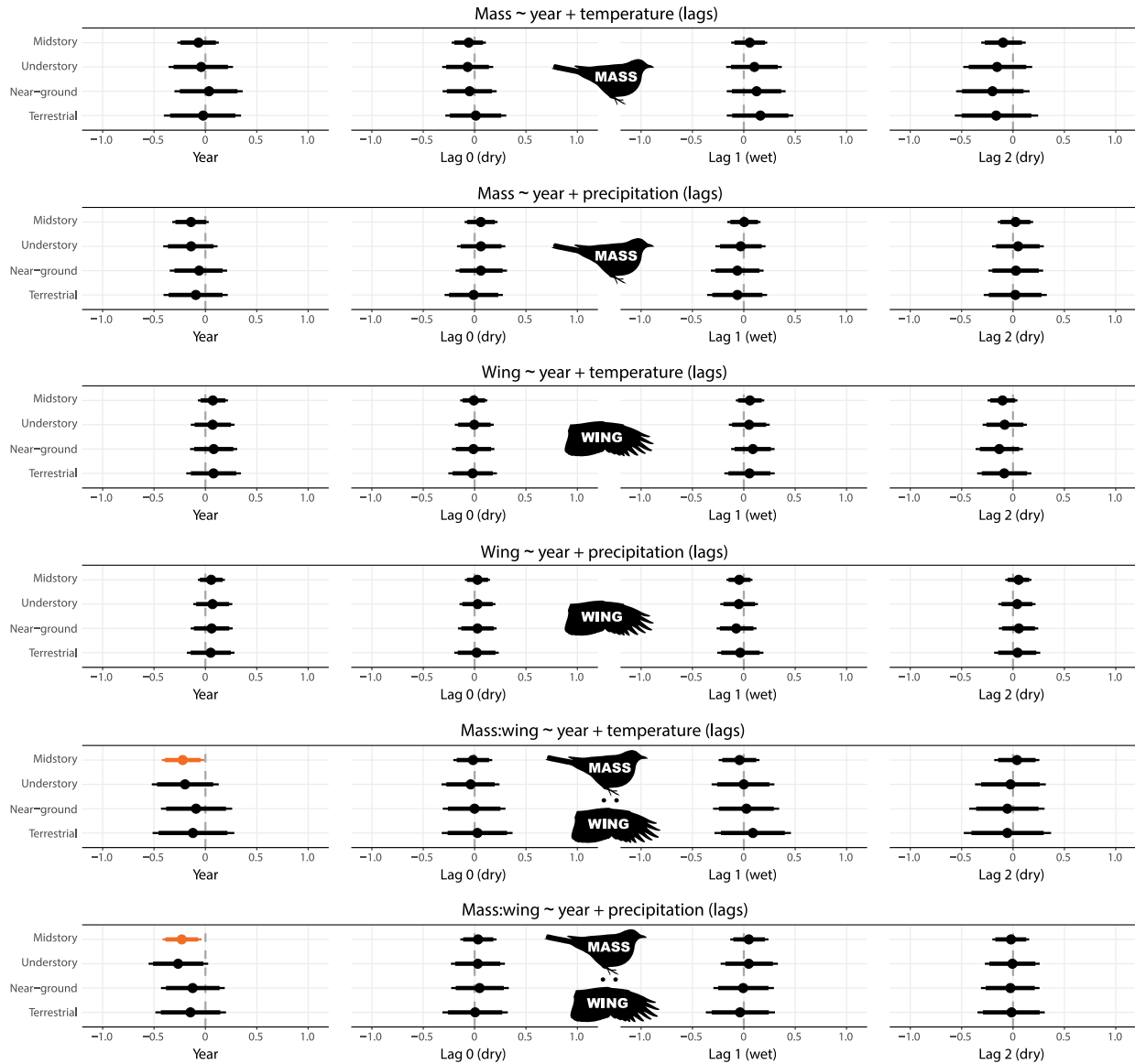


**Fig. S2. Trends in morphology vs abundance.** (A) Morphological trends in Fig. 1D were grouped by foraging guild, with species sorted by mass trends within each guild. Vertical guild position follows guild-specific abundance trends (9). (B–D) Phylogenetic generalized least squares (PGLS) regression between abundance and morphology trends. Results correspond to models 1, 7, 13 (table S4).











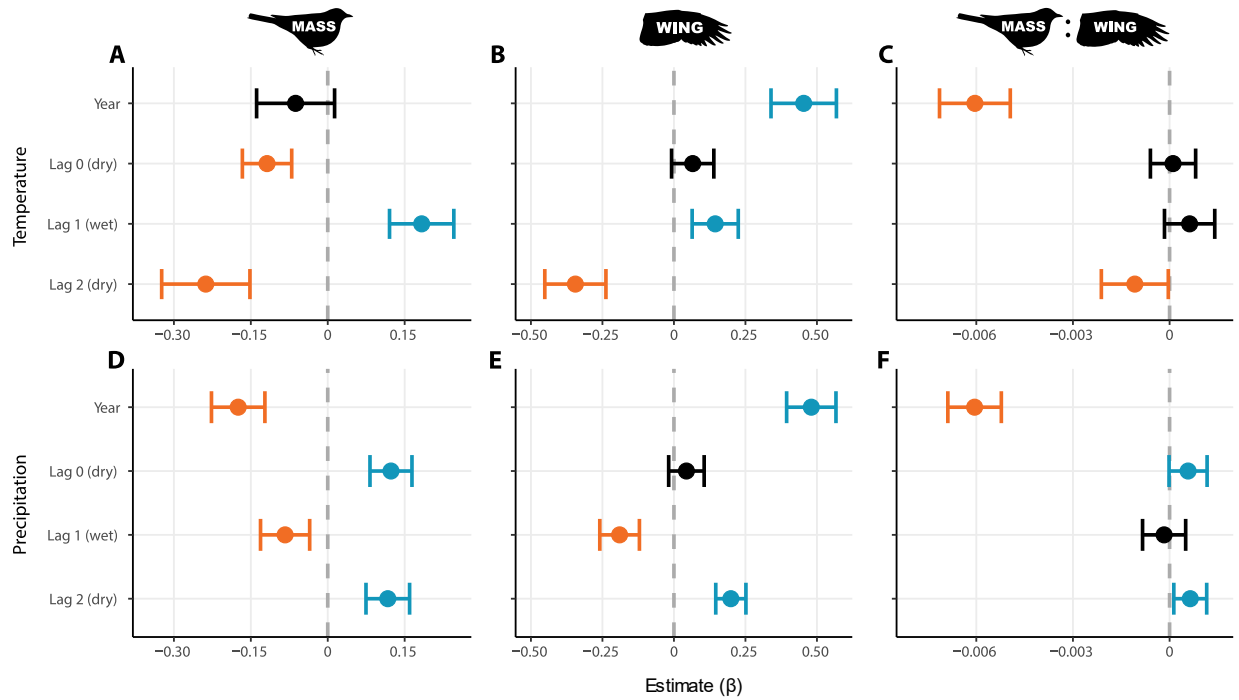












**Fig. S3. Morphological responses of bird foraging guild to year and climate.** Points are Gamma parameter estimates from the second level of a hierarchical model of individual species trends, indicating the overall estimated response of a given group of species to each covariate. Lines represent 90% and 95% credible intervals. Plots show Gamma values for models depicted in Fig. 4. Guilds are sorted according to abundance trends (9). Results correspond to models 2, 3, 8, 9, 14, and 15 (table S4).



**Fig. S4. Morphological responses of bird forest stratum to year and climate.** Points are Gamma parameter estimates from the second level of a hierarchical model of individual species trends, indicating the overall estimated response of a given group of species to each covariate. Lines represent 90% and 95% credible intervals. Plots show Gamma values for models identical to Fig. 4, with stratum (rather than guild) as the species trait. Strata are sorted from low to high. Results correspond to models 5, 6, 11, 12, 17, and 18 (table S4).



**Fig. S5. Bird morphology modeled by time trend and climate covariates using linear mixed models.** Models are fit by restricted maximum likelihood to the entire merged dataset and include random effects of species and month. Predictors are scaled to allow comparison across each morphological metric.

Scenario	MASS	WING	MASS : WING	Flap rate to maintain lift	Caloric demand of flight	Metabolic heat in flight
1) Baseline			2:2 = 1	baseline	baseline	baseline
2) Mass decreases			1:2 = 0.5	lower	lower	lower
3) Wing decreases			2:1 = 2	higher	higher	higher
4) Mass increases			3:2 = 1.5	high	high	high
5) Wing increases			2:3 = 0.67	low	low	low
6) Both increase			3:3 = 1	baseline	baseline	baseline
7) Both decrease			1:1 = 1	baseline	baseline	baseline
8) Mass increase Wing decrease			3:1 = 3	highest	highest	highest
9) Mass decrease Wing increase			1:3 = 0.33	lowest	lowest	lowest

**Fig. S6. Concept map for the consequences of morphological changes on avian energetics.** Out of the scenarios that reduce mass:wing (two, five, nine) from a hypothetical 4-unit energy baseline (scenario one: 2 in mass + 2 in wing), scenario nine is the most economical—scenario two wastes 1 unit, scenario five costs 1 unit, but the net energy requirement for scenario nine is zero. Caloric demand of flight is based on (40).



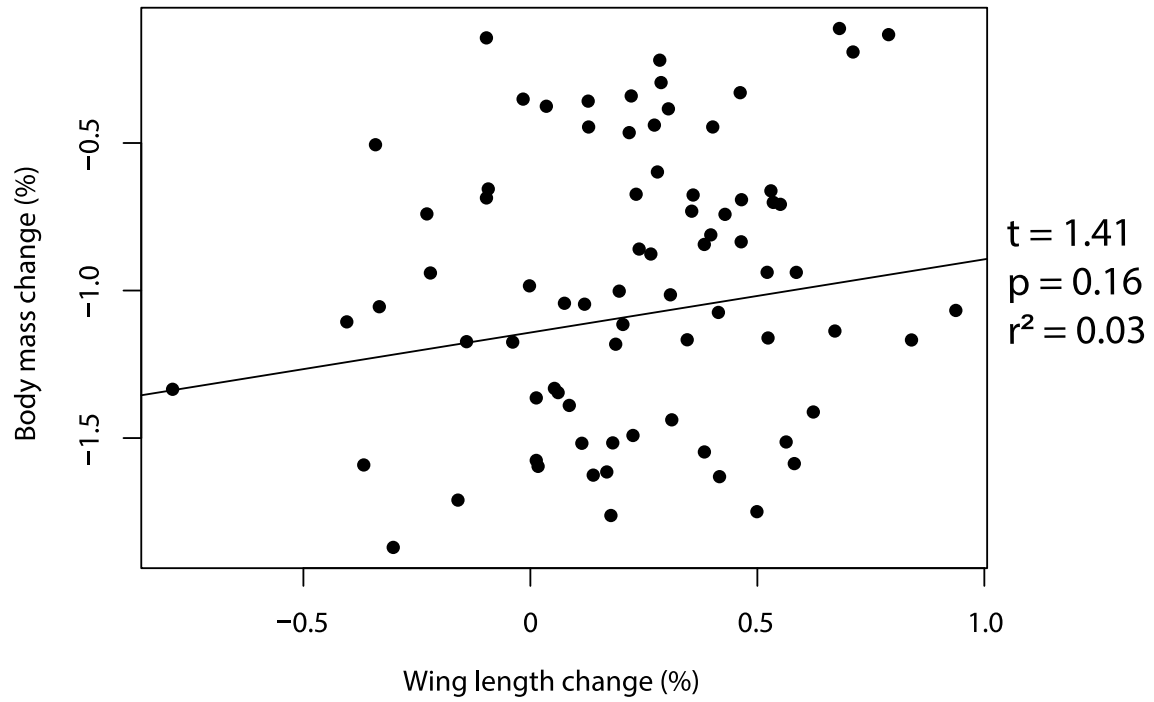


**Fig. S7. Correlation between mass and wing change.** Regression is based on phylogenetic generalized least squares (PGLS). Results correspond to models 1 and 7 (table S4).

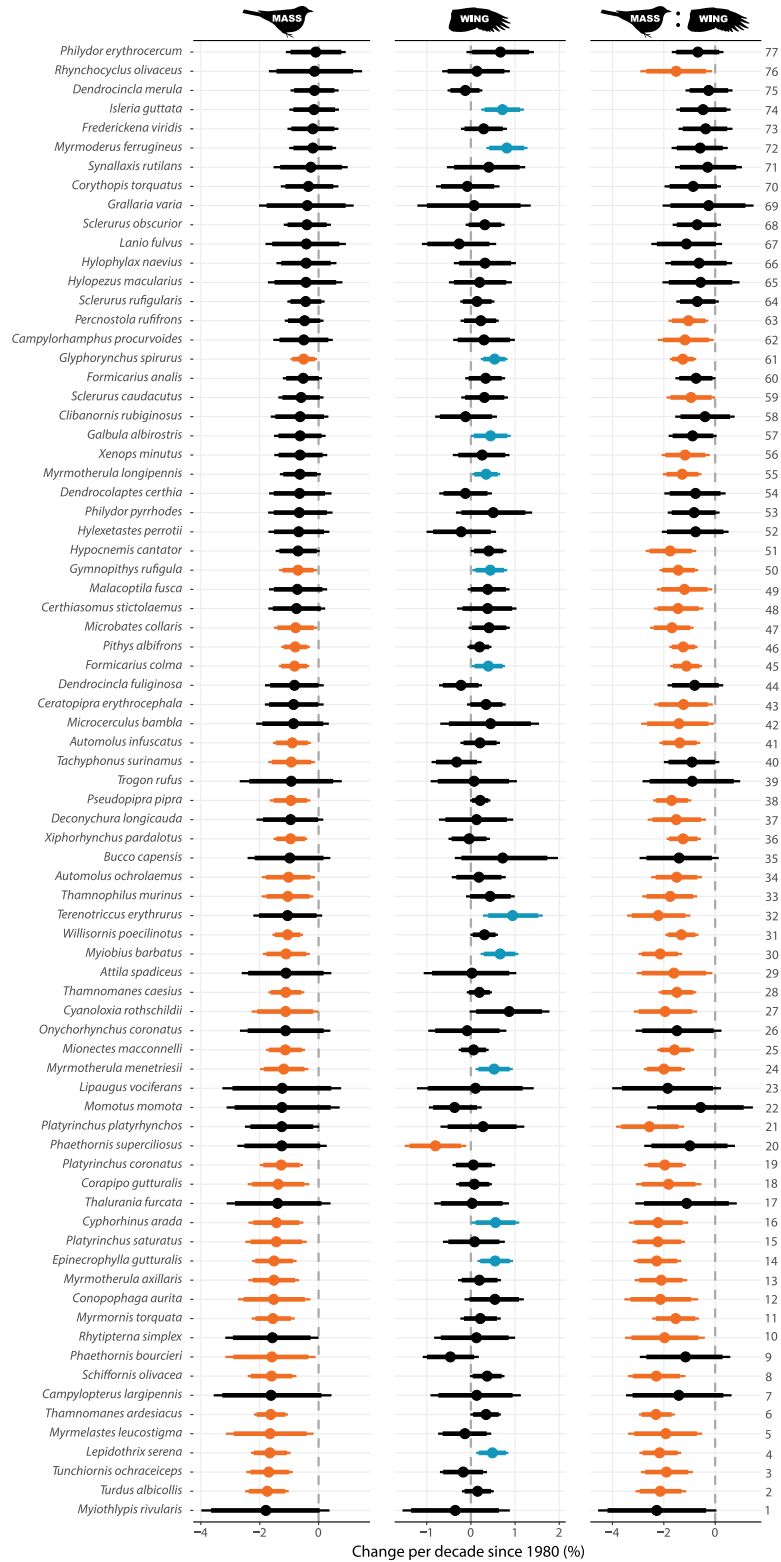


**Fig. S8. HMSC models of morphological trends with a random effect of year.** Model structures are identical to Fig. 1D, but a random effect of categorical year is also included here.

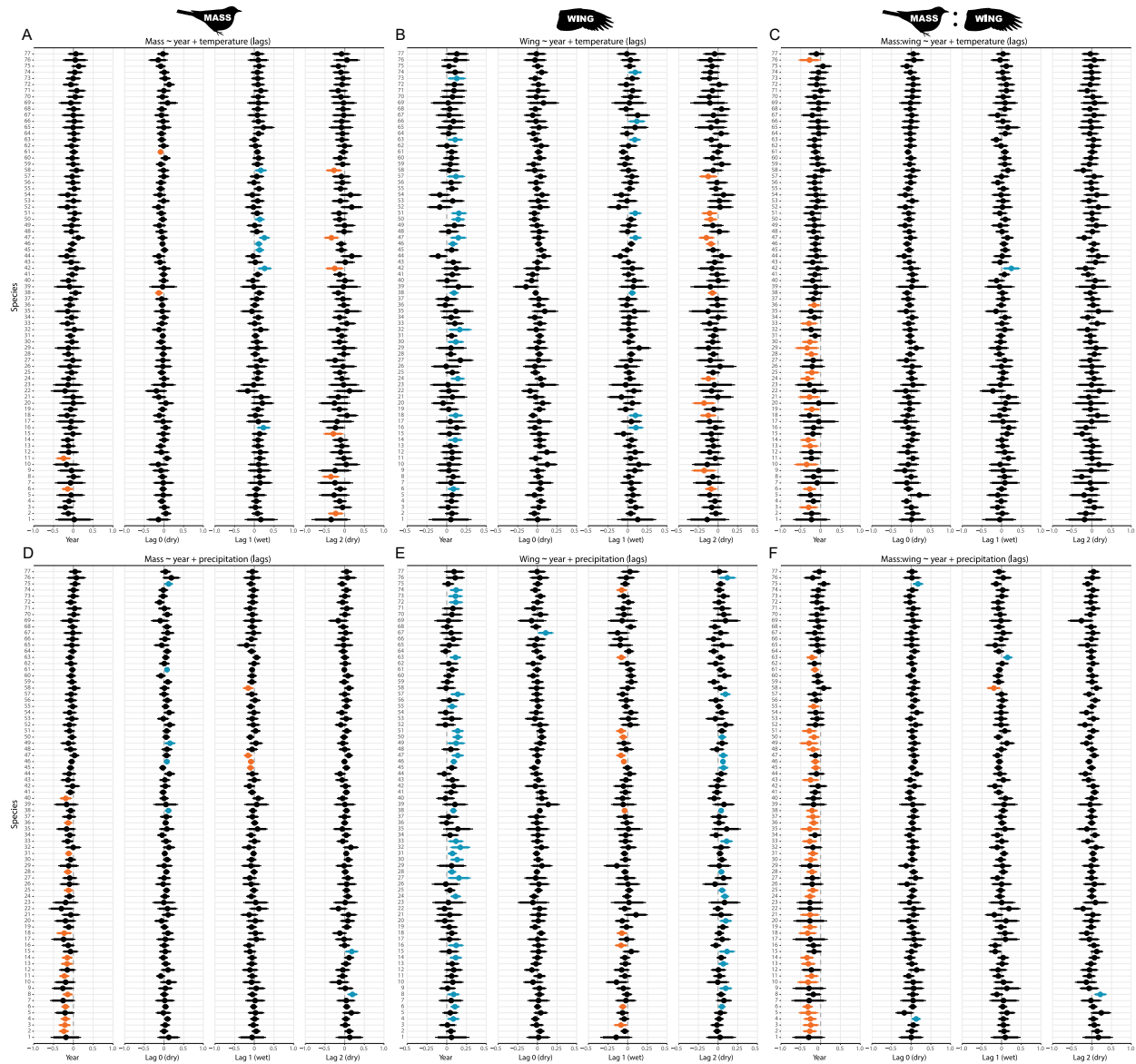


**Fig. S9. Morphology by species modeled by time trend and climate covariates with a random effect of year.** Model structures are identical to Fig. 4, but a random effect of categorical year is also included here.

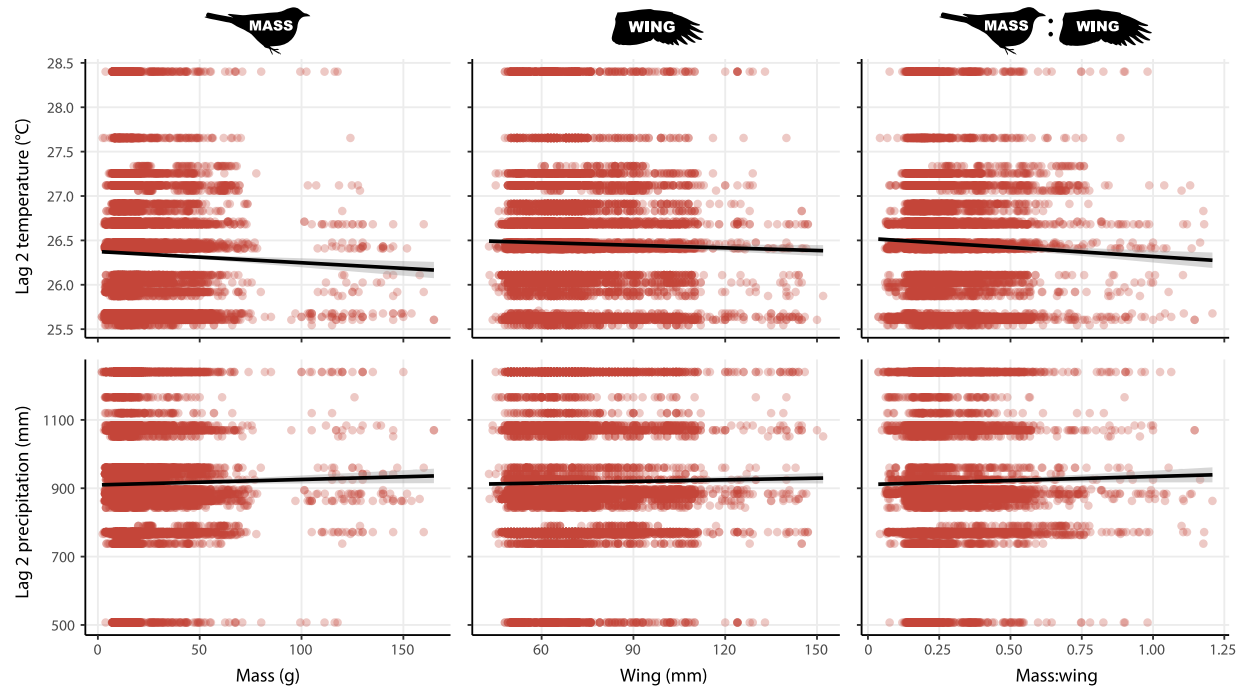


**Fig. S10. Raw morphology and lag 2 climate scatterplots.** Black lines and ribbons represent best-fit linear regressions and 95% CIs for their predictions. The most severe season (28.4 °C, 507 mm) corresponds to the widespread drought in 2016 (84).

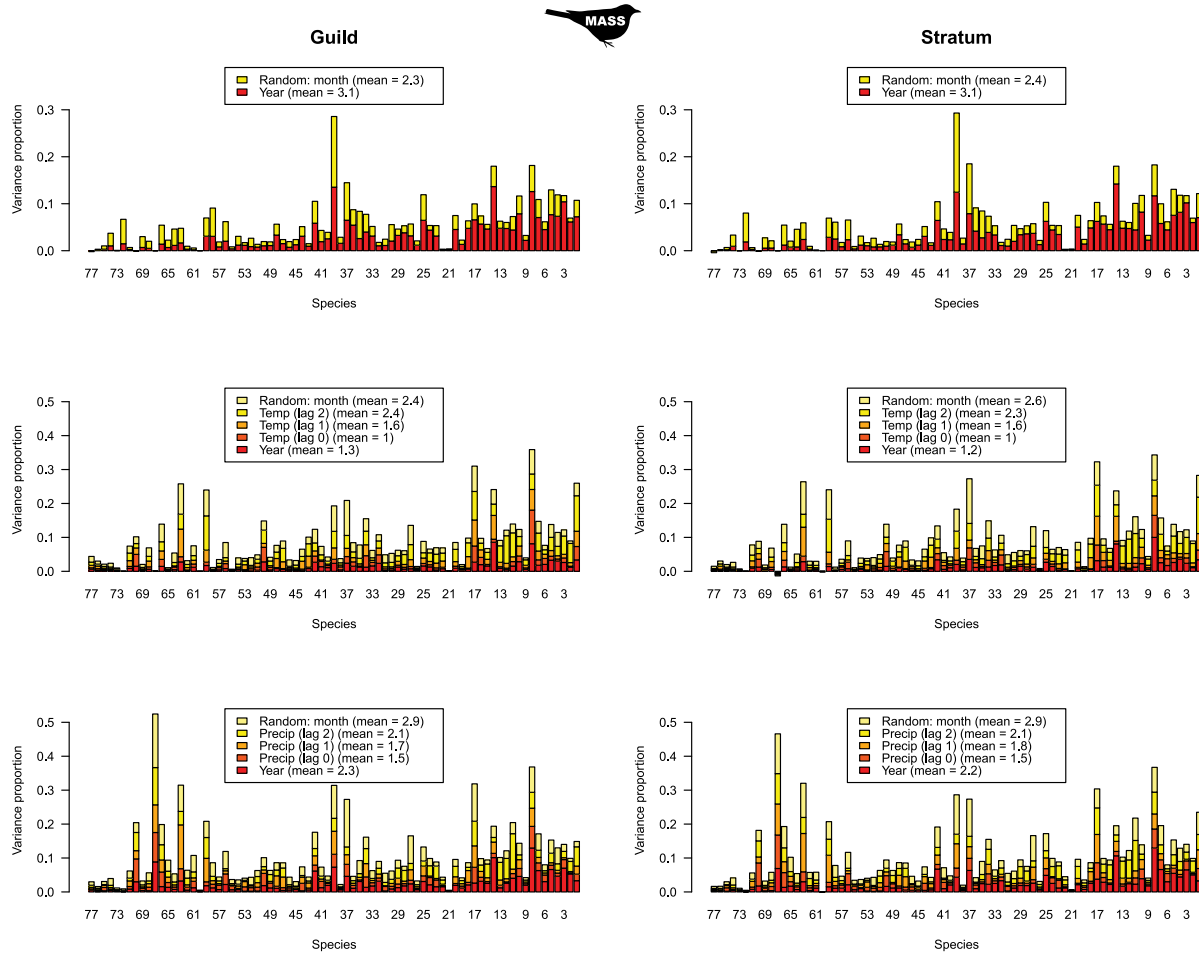


**Fig. S11. Variance partitioning for mass models.** Vertical bars show the proportion of variance explained by each covariate, corrected for each species'  $R^2$  value for a given model. Legends show mean proportion for each covariate. For more details, see models 1–6 in Table S4. Species are ordered on the x-axis following declining mass in Fig. 1D.

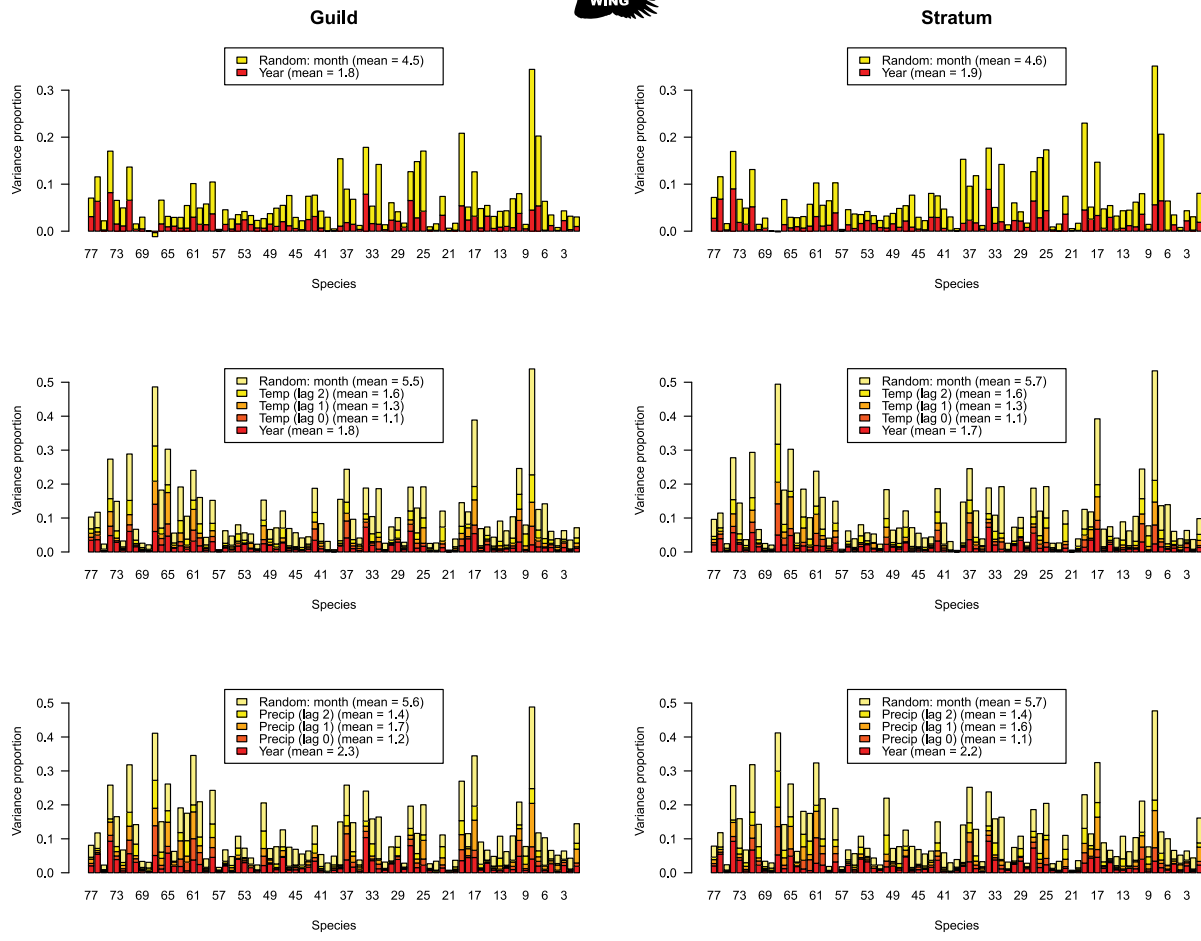


**Fig. S12. Variance partitioning for wing models.** Vertical bars show the proportion of variance explained by each covariate, corrected for each species'  $R^2$  value for a given model. Legends show mean proportion for each covariate. For more details, see models 7–12 in Table S4. Species are ordered on the x-axis following declining mass in Fig. 1D.



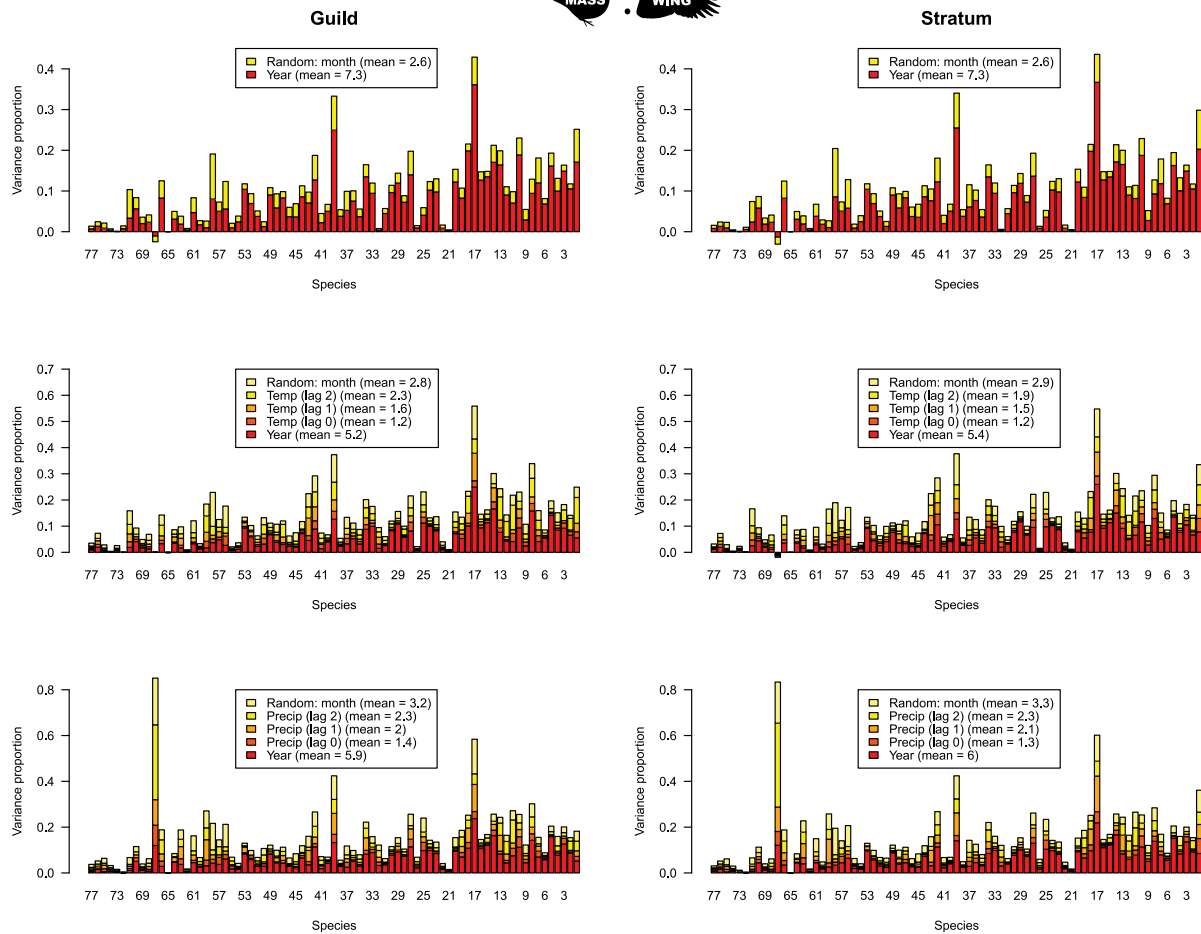


**Fig. S13. Variance partitioning for mass:wing models.** Vertical bars show the proportion of variance explained by each covariate, corrected for each species'  $R^2$  value for a given model. Legends show mean proportion for each covariate. For more details, see models 13–18 in Table S4. Species are ordered on the x-axis following declining mass in Fig. 1D.

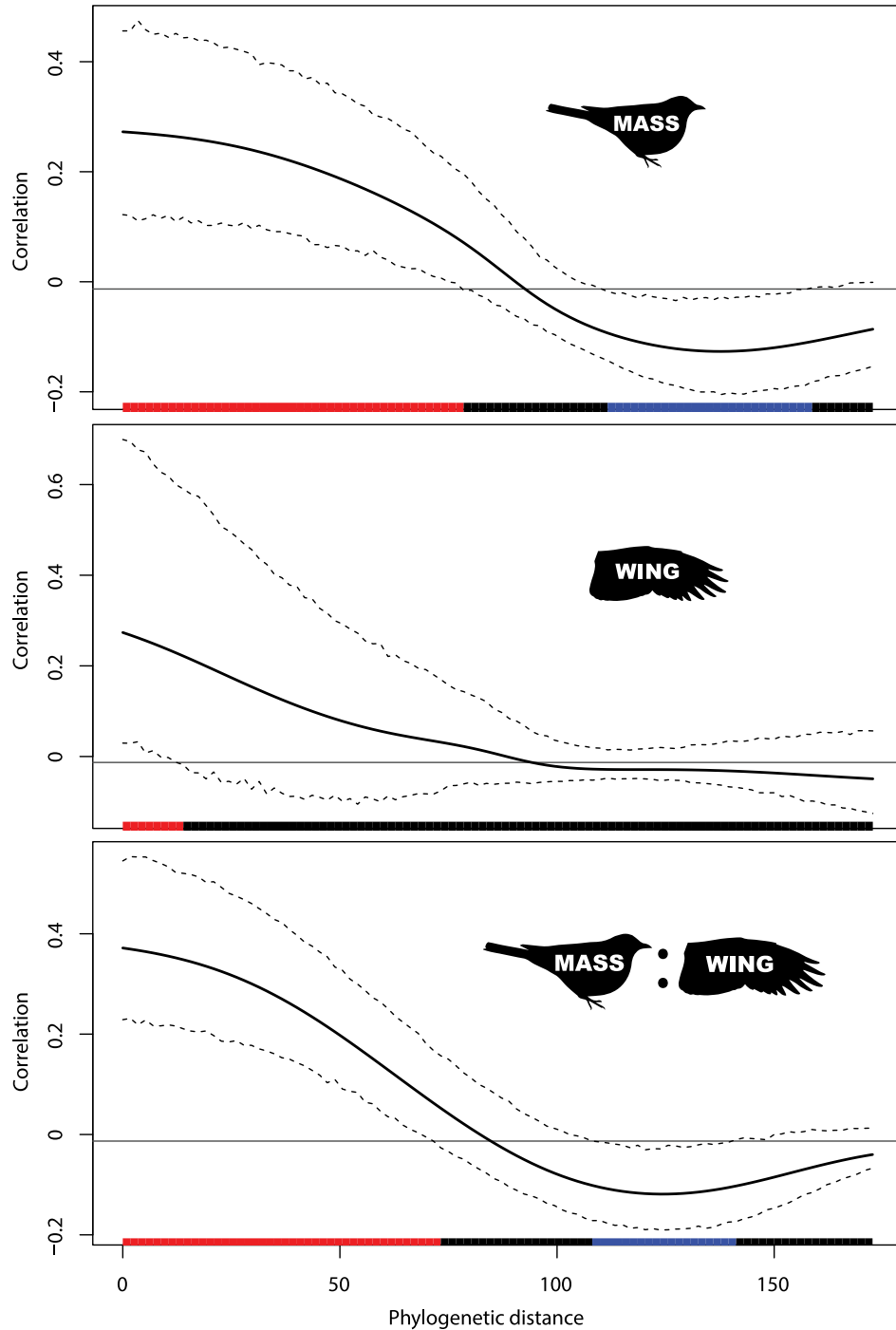


**Fig. S14. Phylogenetic correlation in morphological changes through time.** The bold black line represents Moran's I, an index of autocorrelation, compared to the null hypothesis (solid horizontal line). Dashed lines represent 95% confidence intervals, based on nonparametric bootstrap resampling. Colored x-axis bars show regions of significant positive (red) and negative (blue) autocorrelation. Plots were created using the *phylosignal* R package (77). Morphological change estimates are from models 1, 7, and 13 (table S4).

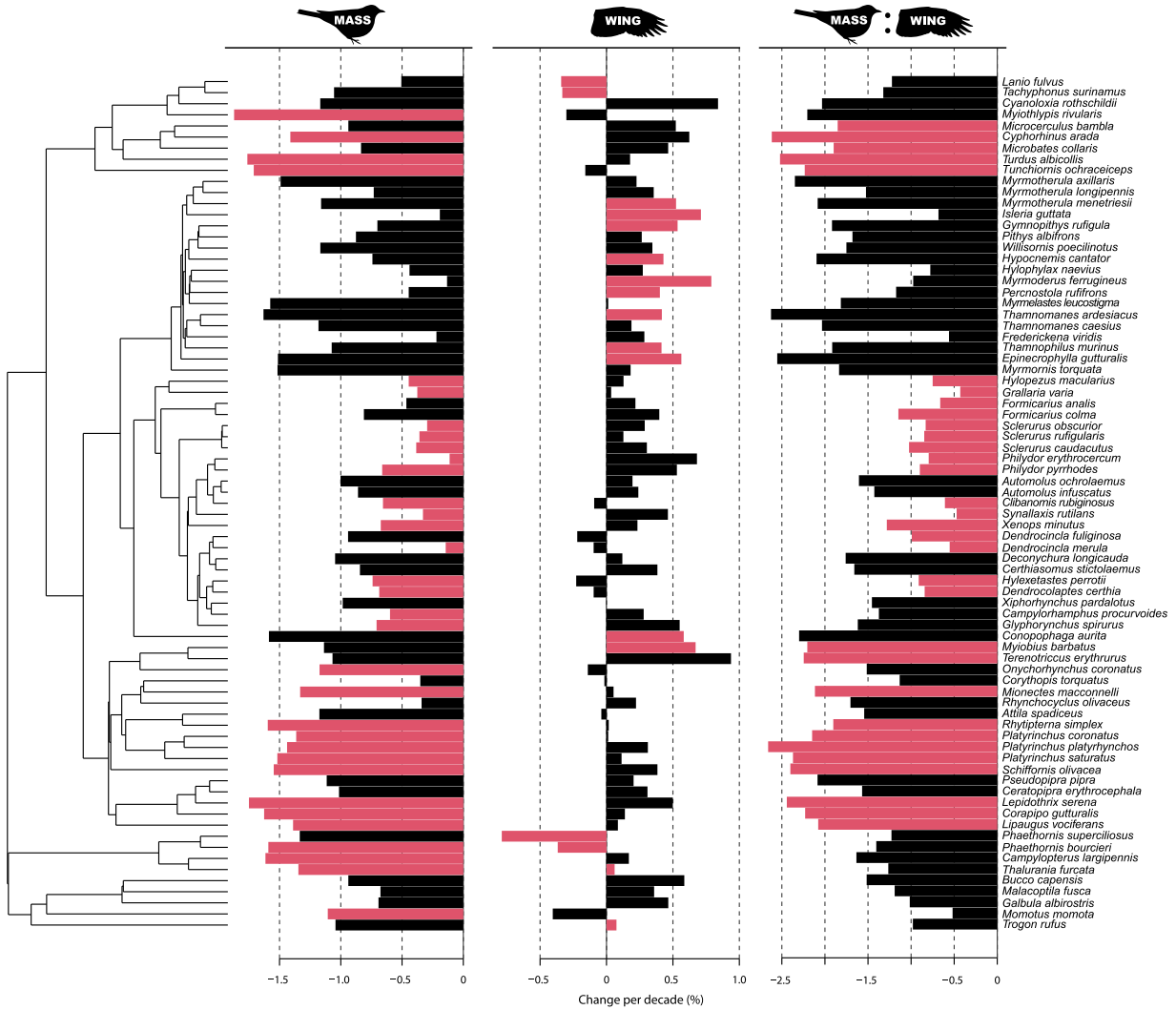


**Fig. S15. Phylogenetic correlation in species-specific morphological change over time.** Bars show median rate of change per decade, as a percentage of model-estimated median 1980 mass, wing length, or mass:wing ratio. Red bars indicate species with values more similar to their neighbors than expected by chance, meaning that the local indicator of phylogenetic association (LIPA; local Moran's I) is significantly positive ( $p < 0.05$ ) based on permutation tests. Phylogenetic tree is from [birdtree.org](http://birdtree.org) (74). Plots were created using the *phylosignal* R package (77). Morphological change estimates are from models 1, 7, and 13 (table S4).

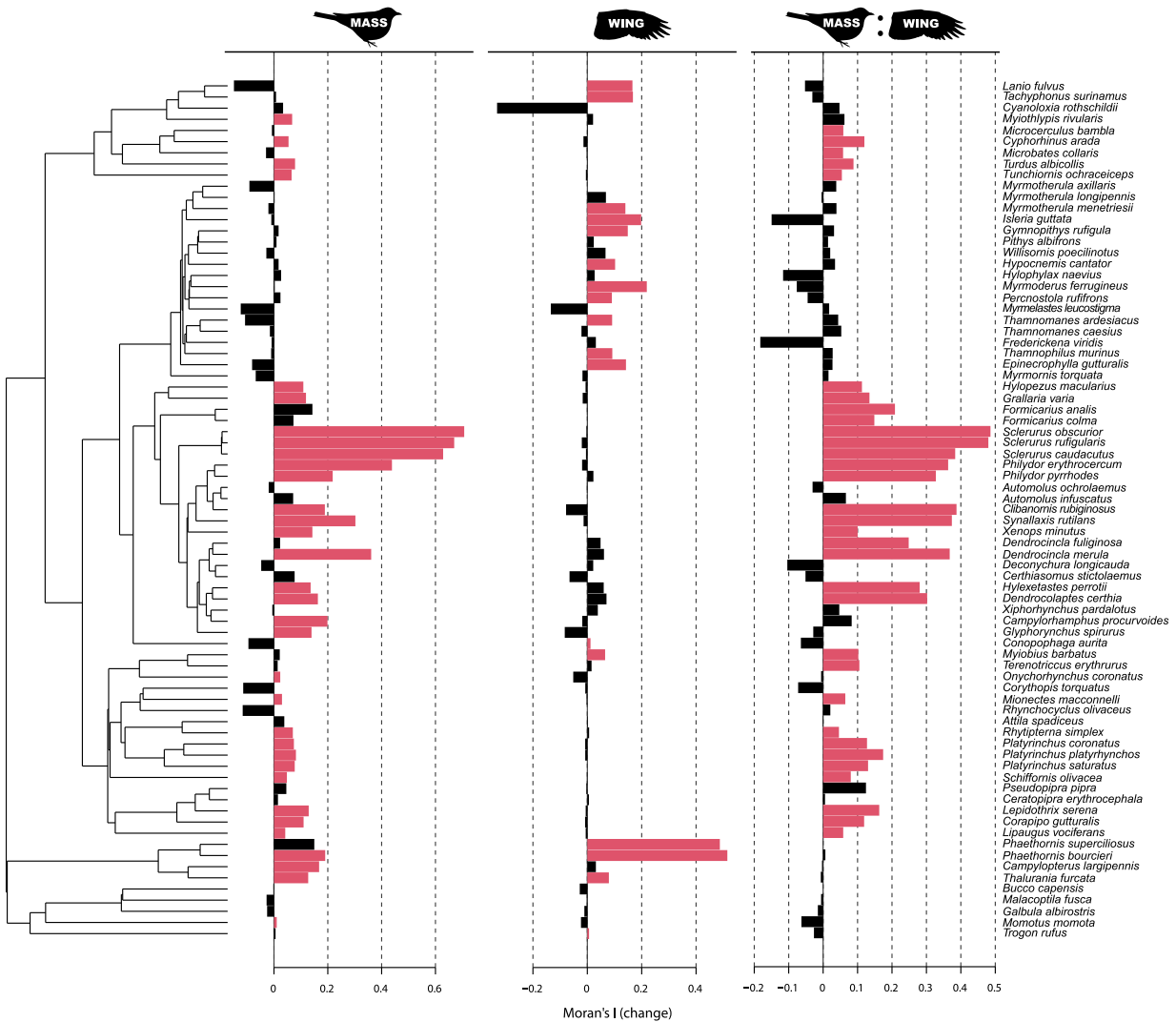


**Fig. S16. Phylogenetic correlation in species-specific morphological change over time: Moran's I.** Bars show the local indicator of phylogenetic association (LIPA; local Moran's I) for each species. Red bars indicate species with values more similar to their neighbors than expected by chance, meaning that the local Moran's I for that species is significantly positive ( $p < 0.05$ ) based on permutation tests. Phylogenetic tree is from [birdtree.org](http://birdtree.org) (74). Plots were created using the *phylosignal* R package (77). Morphological change estimates are from models 1, 7, and 13 (table S4).

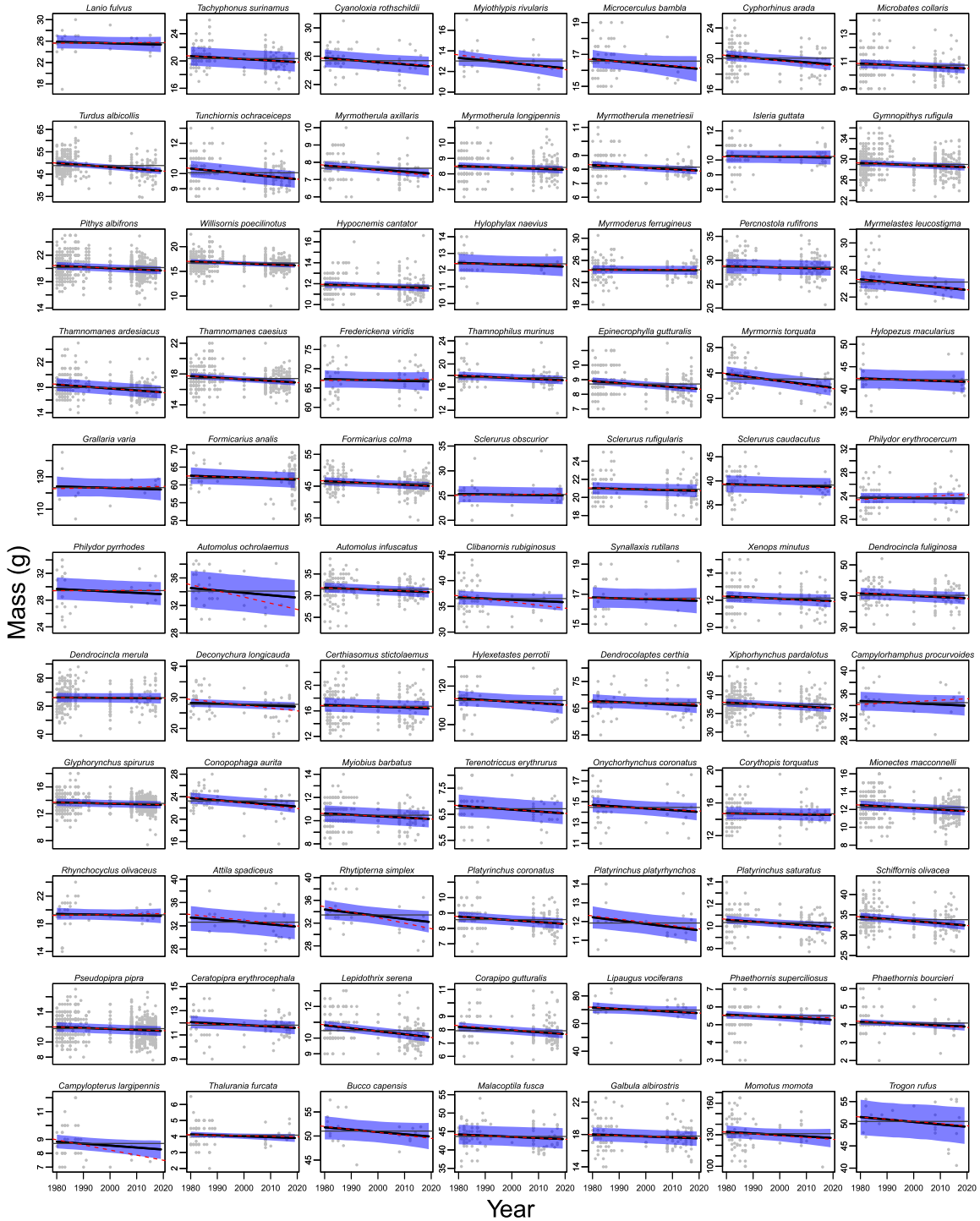


**Fig. S17. Time trends in mass by species.** Points show raw data values. Solid black line represents the median estimate of mass trend with 95% credible interval ribbon from an HMSC model including phylogeny and foraging guild (model 1 in Table S4). Dashed red line is a simple linear model for that species. Gray horizontal line is the overall mean value for that species.



WING

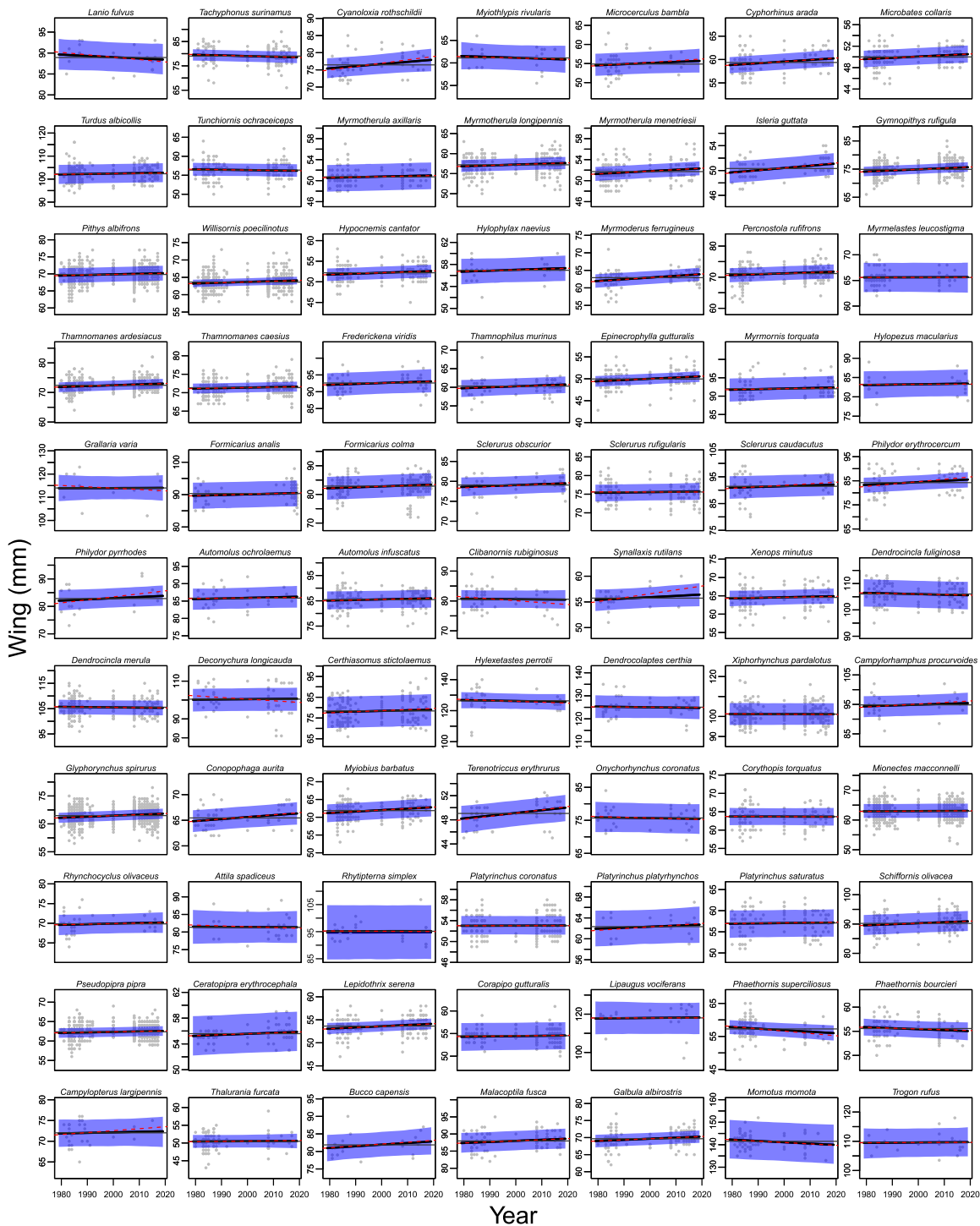


**Fig. S18. Time trends in wing length by species.** Points show raw data values. Solid black line represents the median estimate of wing trends with 95% credible interval ribbon from an HMSC model including phylogeny and foraging guild (model 7 in Table S4). Dashed red line is a simple linear model for that species. Gray horizontal line is the overall mean value for that species.

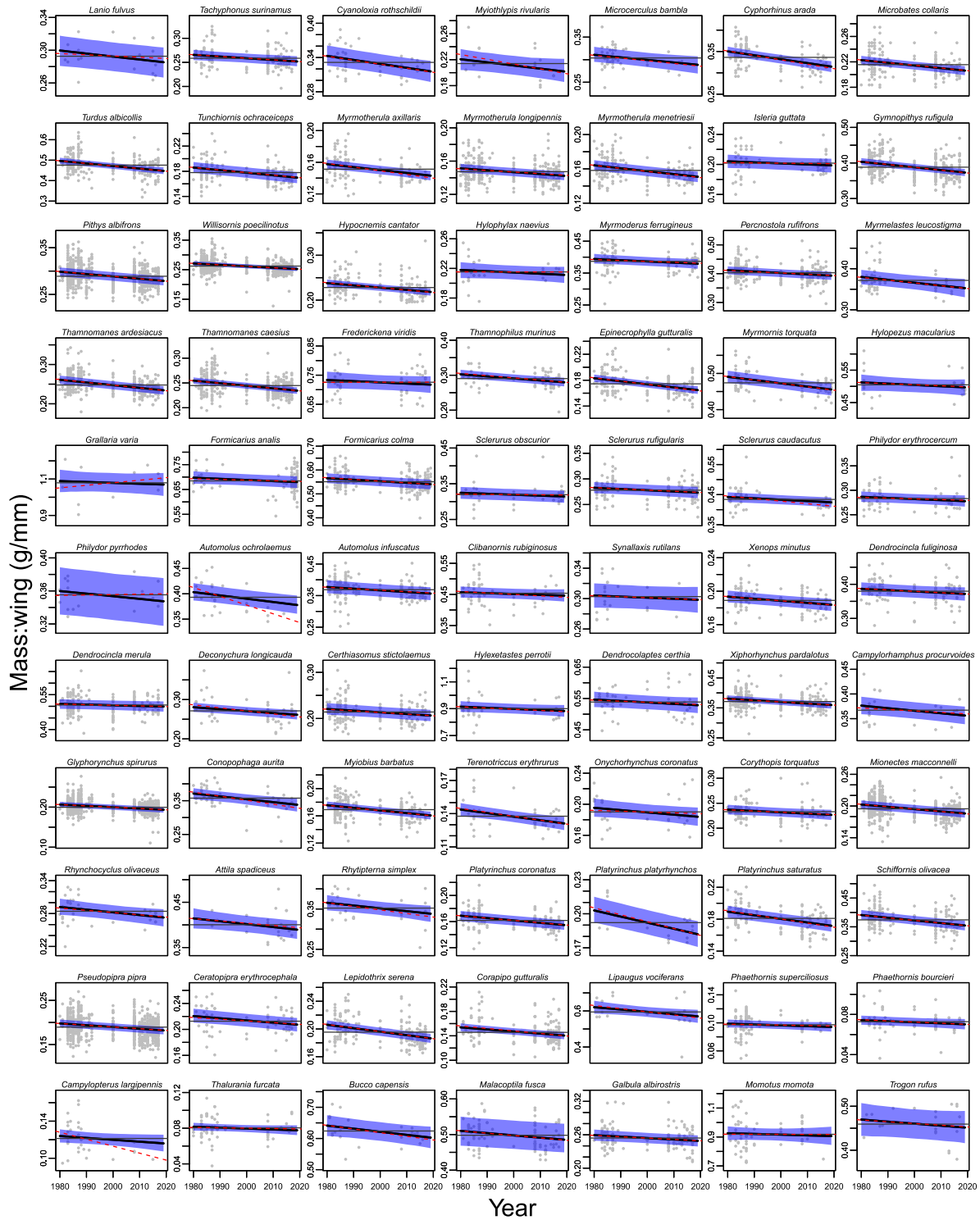


**Fig. S19. Time trends in mass:wing by species.** Points show raw data values. Solid black line represents the median estimate with 95% credible interval ribbon from an HMSC model including phylogeny and foraging guild (model 13 in Table S4). Dashed red line is a simple linear model for that species. Gray horizontal line is the overall mean value for that species.

**Table S1. Time trend of bird morphology examined using linear mixed models.** Models are fit with maximum likelihood to the entire dataset and include species and month as random effects. Significance of the time-trend parameter (year) is assessed using the Satterthwaite's method.

<i>Predictors</i>	<b>Mass</b>				<b>Wing</b>				<b>Mass:wing</b>			
	<i>Estimates</i>	<i>CI</i>	<i>Statistic</i>	<i>p</i>	<i>Estimates</i>	<i>CI</i>	<i>Statistic</i>	<i>p</i>	<i>Estimates</i>	<i>CI</i>	<i>Statistic</i>	<i>p</i>
(Intercept)	69.28	61.52 – 77.03	17.50	<0.001	39.17	30.18 – 48.15	8.55	<0.001	1.30	1.21 – 1.38	29.83	<0.001
Year	-0.02	-0.02 – -0.02	-14.79	<0.001	0.02	0.01 – 0.02	9.23	<0.001	-0.00	-0.00 – -0.00	-25.57	<0.001
Random Effects												
$\sigma^2$	5.29				7.61				0.00			
$\tau_{00}$	611.75 <sub>species</sub>				424.61 <sub>species</sub>				0.04 <sub>species</sub>			
	0.00 <sub>month</sub>				0.00 <sub>month</sub>				0.00 <sub>month</sub>			
ICC	0.99				0.98				0.98			
<i>n</i>	77 <sub>species</sub>				77 <sub>species</sub>				77 <sub>species</sub>			
	6 <sub>month</sub>				6 <sub>month</sub>				6 <sub>month</sub>			
Observations	14842				11582				11009			
Marginal R <sup>2</sup> / Conditional R <sup>2</sup>	0.000 / 0.991				0.000 / 0.982				0.001 / 0.982			
AIC	67578.121				57036.770				-48878.082			

**Table S2. Bird morphology modeled by time trend and lagged seasonal temperature using linear mixed models.** Models are fit with maximum likelihood to the entire dataset and include species and month as random effects. Significance of parameters is assessed using the Satterthwaite's method.

<i>Predictors</i>	<b>Mass</b>				<b>Wing</b>				<b>Mass:wing</b>			
	<i>Estimates</i>	<i>CI</i>	<i>Statistic</i>	<i>p</i>	<i>Estimates</i>	<i>CI</i>	<i>Statistic</i>	<i>p</i>	<i>Estimates</i>	<i>CI</i>	<i>Statistic</i>	<i>p</i>
(Intercept)	42.87	31.89 – 53.85	7.65	<0.001	14.81	-0.22 – 29.84	1.93	0.053	1.21	1.06 – 1.35	16.41	<0.001
Year	-0.00	-0.01 – 0.00	-1.62	0.106	0.03	0.02 – 0.04	7.78	<0.001	-0.00	-0.00 – -0.00	-10.79	<0.001
Temp lag 0 (dry)	-0.19	-0.27 – -0.11	-4.83	<0.001	0.10	-0.01 – 0.22	1.74	0.081	0.00	-0.00 – 0.00	0.30	0.766
Temp lag 1 (wet)	0.35	0.23 – 0.47	5.73	<0.001	0.27	0.12 – 0.43	3.51	<0.001	0.00	-0.00 – 0.00	1.56	0.118
Temp lag 2 (dry)	-0.37	-0.50 – -0.24	-5.44	<0.001	-0.53	-0.70 – -0.37	-6.33	<0.001	-0.00	-0.00 – -0.00	-2.04	<b>0.041</b>
Random effects												
$\sigma^2$	5.27				7.57				0.00			
$\tau_{00}$	611.70 <sub>species</sub>				424.31 <sub>species</sub>				0.04 <sub>species</sub>			
	0.00 <sub>month</sub>				0.00 <sub>month</sub>				0.00 <sub>month</sub>			
ICC	0.99				0.98				0.98			
<i>n</i>	77 <sub>species</sub>				77 <sub>species</sub>				77 <sub>species</sub>			
	6 <sub>month</sub>				6 <sub>month</sub>				6 <sub>month</sub>			
Observations	14842				11582				11009			
Marginal R <sup>2</sup> / Conditional R <sup>2</sup>	0.000 / 0.991				0.000 / 0.982				0.001 / 0.982			
AIC	67533.936				56993.767				-48876.644			

**Table S3. Bird morphology modeled by time trend and lagged seasonal precipitation using linear mixed models.** Models are fit with maximum likelihood to the entire dataset and include species and month as random effects. Significance of parameters is assessed using the Satterthwaite's method.

<i>Predictors</i>	<b>Mass</b>				<b>Wing</b>				<b>Mass:wing</b>			
	<i>Estimates</i>	<i>CI</i>	<i>Statistic</i>	<i>p</i>	<i>Estimates</i>	<i>CI</i>	<i>Statistic</i>	<i>p</i>	<i>Estimates</i>	<i>CI</i>	<i>Statistic</i>	<i>p</i>
(Intercept)	52.18	42.93 – 61.44	11.06	<b>&lt;0.001</b>	6.45	-6.80 – 19.70	0.95	0.340	1.19	1.07 – 1.32	18.43	<b>&lt;0.001</b>
Year	-0.01	-0.02 – -0.01	-6.58	<b>&lt;0.001</b>	0.03	0.03 – 0.04	10.92	<b>&lt;0.001</b>	-0.00	-0.00 – -0.00	-14.29	<b>&lt;0.001</b>
Precip lag 0 (dry)	0.00	0.00 – 0.00	5.90	<b>&lt;0.001</b>	0.00	-0.00 – 0.00	1.38	0.168	0.00	-0.00 – 0.00	1.91	0.057
Precip lag 1 (wet)	-0.00	-0.00 – -0.00	-3.40	<b>0.001</b>	-0.00	-0.00 – -0.00	-5.38	<b>&lt;0.001</b>	-0.00	-0.00 – 0.00	-0.50	0.619
Precip lag 2 (dry)	0.00	0.00 – 0.00	5.44	<b>&lt;0.001</b>	0.00	0.00 – 0.00	7.40	<b>&lt;0.001</b>	0.00	0.00 – 0.00	2.47	<b>0.013</b>
Random effects												
$\sigma^2$	5.26				7.56				0.00			
$\tau_{00}$	611.75 <sub>species</sub>				424.44 <sub>species</sub>				0.04 <sub>species</sub>			
	0.00 <sub>month</sub>				0.00 <sub>month</sub>				0.00 <sub>month</sub>			
ICC	0.99				0.98				0.98			
<i>n</i>	77 <sub>species</sub>				77 <sub>species</sub>				77 <sub>species</sub>			
	6 <sub>month</sub>				6 <sub>month</sub>				6 <sub>month</sub>			
Observations	14842				11582				11009			
Marginal R <sup>2</sup> / Conditional R <sup>2</sup>	0.000 / 0.991				0.000 / 0.983				0.001 / 0.982			
AIC	67506.383				56974.802				-48882.735			



**Table S4. Structure and fit of Bayesian joint species models used in this study.** Models 1–18 included the effect of phylogeny and trait. Models 19–27 merge species, which are then treated as a random effect, and do not include phylogeny or trait.

Index	Model	Response variable	Predictor covariates	Trait	Mean R <sup>2</sup>
1	Time	Mass	Year	Guild	0.054
2	Temperature	"	Year + Temp_Lag0 <sub>dry</sub> + Temp_Lag1 <sub>wet</sub> + Temp_Lag2 <sub>dry</sub>	"	0.087
3	Precipitation	"	Year + Precip_Lag0 <sub>dry</sub> + Precip_Lag1 <sub>wet</sub> + Precip_Lag2 <sub>dry</sub>	"	0.105
4	Time	"	Year	Stratum	0.055
5	Temperature	"	Year + Temp_Lag0 <sub>dry</sub> + Temp_Lag1 <sub>wet</sub> + Temp_Lag2 <sub>dry</sub>	"	0.086
6	Precipitation	"	Year + Precip_Lag0 <sub>dry</sub> + Precip_Lag1 <sub>wet</sub> + Precip_Lag2 <sub>dry</sub>	"	0.105
7	Time	Wing	Year	Guild	0.063
8	Temperature	"	Year + Temp_Lag0 <sub>dry</sub> + Temp_Lag1 <sub>wet</sub> + Temp_Lag2 <sub>dry</sub>	"	0.114
9	Precipitation	"	Year + Precip_Lag0 <sub>dry</sub> + Precip_Lag1 <sub>wet</sub> + Precip_Lag2 <sub>dry</sub>	"	0.122
10	Time	"	Year	Stratum	0.066
11	Temperature	"	Year + Temp_Lag0 <sub>dry</sub> + Temp_Lag1 <sub>wet</sub> + Temp_Lag2 <sub>dry</sub>	"	0.114
12	Precipitation	"	Year + Precip_Lag0 <sub>dry</sub> + Precip_Lag1 <sub>wet</sub> + Precip_Lag2 <sub>dry</sub>	"	0.120
13	Time	Mass:wing	Year	Guild	0.099
14	Temperature	"	Year + Temp_Lag0 <sub>dry</sub> + Temp_Lag1 <sub>wet</sub> + Temp_Lag2 <sub>dry</sub>	"	0.131
15	Precipitation	"	Year + Precip_Lag0 <sub>dry</sub> + Precip_Lag1 <sub>wet</sub> + Precip_Lag2 <sub>dry</sub>	"	0.149
16	Time	"	Year	Stratum	0.099
17	Temperature	"	Year + Temp_Lag0 <sub>dry</sub> + Temp_Lag1 <sub>wet</sub> + Temp_Lag2 <sub>dry</sub>	"	0.129
18	Precipitation	"	Year + Precip_Lag0 <sub>dry</sub> + Precip_Lag1 <sub>wet</sub> + Precip_Lag2 <sub>dry</sub>	"	0.150
19	Time	Mass	Year	NA	0.026
20	Temperature	"	Year + Temp_Lag0 <sub>dry</sub> + Temp_Lag1 <sub>wet</sub> + Temp_Lag2 <sub>dry</sub>	NA	0.035
21	Precipitation	"	Year + Precip_Lag0 <sub>dry</sub> + Precip_Lag1 <sub>wet</sub> + Precip_Lag2 <sub>dry</sub>	NA	0.041
22	Time	Wing	Year	NA	0.009
23	Temperature	"	Year + Temp_Lag0 <sub>dry</sub> + Temp_Lag1 <sub>wet</sub> + Temp_Lag2 <sub>dry</sub>	NA	0.014
24	Precipitation	"	Year + Precip_Lag0 <sub>dry</sub> + Precip_Lag1 <sub>wet</sub> + Precip_Lag2 <sub>dry</sub>	NA	0.016
25	Time	Mass:wing	Year	NA	0.071
26	Temperature	"	Year + Temp_Lag0 <sub>dry</sub> + Temp_Lag1 <sub>wet</sub> + Temp_Lag2 <sub>dry</sub>	NA	0.072
27	Precipitation	"	Year + Precip_Lag0 <sub>dry</sub> + Precip_Lag1 <sub>wet</sub> + Precip_Lag2 <sub>dry</sub>	NA	0.074

**Table S5. Bird morphology by age.** Models are linear mixed models with species as a random effect fit with restricted maximum likelihood. Significance of age group effect (juvenile) is assessed using the Satterthwaite's method.

<i>Predictors</i>	<b>Mass</b>				<b>Wing</b>				<b>Mass:wing</b>			
	<i>Estimates</i>	<i>CI</i>	<i>Statistic</i>	<i>p</i>	<i>Estimates</i>	<i>CI</i>	<i>Statistic</i>	<i>p</i>	<i>Estimates</i>	<i>CI</i>	<i>Statistic</i>	<i>p</i>
(Intercept)	28.16	22.47 – 33.86	9.70	<0.001	75.77	71.16 – 80.39	32.18	<0.001	0.33	0.29 – 0.37	14.85	<0.001
Juvenile	-0.45	-0.58 – -0.33	-7.06	<0.001	-0.59	-0.76 – -0.43	-7.08	<0.001	-0.00	-0.01 – -0.00	-5.33	<0.001
Random effects												
$\sigma^2$	4.36				6.50				0.00			
$\tau_{00}$	649.02	species			426.56	species			0.04	species		
ICC	0.99				0.98				0.99			
<i>n</i>	77	species			77	species			77	species		
Observations	7362				6192				5927			
Marginal R <sup>2</sup> / Conditional R <sup>2</sup>	0.000 / 0.993				0.000 / 0.985				0.000 / 0.985			

**Table S6. Bird species considered in analysis, their trait assignments, and model-estimated body mass, wing length, and mass:wing ratio.** Taxonomy follows South American Checklist Committee ver. 9 Feb 21. Morphological change estimates are from models 1, 7, and 13 (table S4).

Species	Guild	Stratum	Mass (g)				Wing length (mm)				Mass:wing ratio			
			<i>n</i>	1980	2019	Δ (%)	<i>n</i>	1980	2019	Δ (%)	<i>n</i>	1980	2019	Δ (%)
TROCHILIDAE														
<i>Phaethornis bourcierii</i>	HU	U	115	4.16	3.90	-6.20 ▼	95	55.85	55.05	-1.43	74	0.07	0.07	-5.41
<i>Phaethornis superciliosus</i>	HU	U	149	5.57	5.28	-5.20	131	57.76	55.99	-3.07 ▼	113	0.10	0.10	-4.04
<i>Campylopterus largipennis</i>	HU	M	45	8.85	8.30	-6.30	36	71.89	72.37	0.66	34	0.12	0.12	-6.45
<i>Thalurania furcata</i>	HU	M	116	4.14	3.93	-5.24	87	50.40	50.52	0.24	69	0.08	0.08	-4.94
TROGONIDAE														
<i>Trogon rufus</i>	MF	M	24	51.63	49.53	-4.07	24	109.48	109.80	0.29	20	0.47	0.45	-3.85
MOMOTIDAE														
<i>Momotus momota</i>	MF	M	80	133.00	127.26	-4.31	68	142.42	140.17	-1.58	60	0.93	0.91	-2.05
GALBULIDAE														
<i>Galbula albirostris</i>	MI	M	167	18.03	17.54	-2.70	140	69.06	70.31	1.81 ▲	134	0.26	0.25	-3.86 ▼
BUCCONIDAE														
<i>Bucco capensis</i>	MI	M	22	51.81	49.92	-3.66	22	81.06	82.91	2.28	22	0.64	0.60	-5.94 ▼
<i>Malacoptila fusca</i>	UI	U	115	44.15	42.98	-2.64	95	87.36	88.59	1.40	91	0.51	0.49	-4.70 ▼
THAMNOPHILIDAE														
<i>Frederickena viridis</i>	NGI	NG	59	67.35	66.77	-0.86	56	91.97	92.99	1.11	51	0.73	0.72	-2.18
<i>Thamnophilus murinus</i>	MI	M	100	17.98	17.22	-4.19 ▼	72	59.85	60.82	1.62	70	0.30	0.28	-7.28 ▼
<i>Thamnomanes ardesiacus</i>	UI	U	508	18.42	17.25	-6.36 ▼	395	71.78	72.95	1.62 ▲	382	0.26	0.23	-10.34 ▼
<i>Thamnomanes caesius</i>	MI	M	504	17.71	16.90	-4.61 ▼	373	71.01	71.53	0.73	356	0.26	0.23	-8.24 ▼
<i>Isleria guttata</i>	NGI	NG	105	10.27	10.19	-0.75	71	49.70	51.08	2.77 ▲	64	0.20	0.20	-2.46
<i>Epinecrophylla gutturalis</i>	UI	U	292	8.89	8.36	-5.91 ▼	205	49.47	50.56	2.20 ▲	194	0.18	0.17	-9.84 ▼
<i>Myrmotherula axillaris</i>	UI	U	165	7.81	7.35	-5.82 ▼	120	50.50	50.95	0.88	114	0.16	0.14	-9.49 ▼
<i>Myrmotherula longipennis</i>	UI	U	370	8.51	8.27	-2.86 ▼	317	56.82	57.61	1.39 ▲	299	0.15	0.14	-5.96 ▼
<i>Myrmotherula menetriesii</i>	MI	M	212	8.31	7.93	-4.53 ▼	182	51.27	52.32	2.04 ▲	171	0.16	0.15	-7.93 ▼

<i>Hypocnemis cantator</i>	GI	U	283	11.94	11.59	-2.90	▼	197	51.62	52.48	1.67	▲	191	0.24	0.22	-7.98	▼	
<i>Percnostola rufifrons</i>	GI	NG	282	28.76	28.26	-1.73		234	70.68	71.79	1.57	▲	220	0.41	0.39	-4.60	▼	
<i>Myrmelastes leucostigma</i>	RI	NG	74	24.64	23.13	-6.14	▼	66	65.76	65.79	0.05		59	0.38	0.35	-7.09	▼	
<i>Myrmoderus ferrugineus</i>	TI	T	147	24.34	24.21	-0.52		107	61.95	63.85	3.08	▲	104	0.39	0.38	-3.82	▼	
<i>Myrmornis torquata</i>	TI	T	101	44.90	42.25	-5.91	▼	77	91.78	92.43	0.71		76	0.49	0.46	-7.14	▼	
<i>Pithys albifrons</i>	AF	NG	1160	20.39	19.70	-3.42	▼	874	69.46	70.18	1.04	▲	831	0.30	0.28	-6.38	▼	
<i>Gymnopithys rufigula</i>	AF	NG	551	29.26	28.46	-2.74	▼	367	74.04	75.58	2.09	▲	351	0.40	0.37	-7.44	▼	
<i>Hylophylax naevius</i>	NGI	NG	43	12.42	12.21	-1.72		28	56.69	57.29	1.07		26	0.22	0.21	-2.75		
<i>Willisornis poecilinotus</i>	NGI	NG	774	16.98	16.21	-4.55	▼	589	63.18	64.03	1.35	▲	566	0.27	0.25	-7.01	▼	
CONOPOPHAGIDAE																		
<i>Conopophaga aurita</i>	NGI	NG	66	23.71	22.25	-6.19	▼	52	64.85	66.32	2.27	▲	49	0.37	0.34	-8.89	▼	
GRALLARIIDAE																		
<i>Grallaria varia</i>	TI	T	12	124.13	122.32	-1.46		12	113.52	113.67	0.14		11	1.09	1.07	-1.65		
<i>Hylopezus macularius</i>	TI	T	30	42.39	41.65	-1.74		24	83.07	83.48	0.50		22	0.51	0.50	-2.93		
FORMICARIIDAE																		
<i>Formicarius colma</i>	TI	T	248	46.52	45.05	-3.16	▼	219	82.16	83.44	1.55	▲	202	0.57	0.54	-4.42	▼	
<i>Formicarius analis</i>	TI	T	98	62.53	61.40	-1.81		100	89.63	90.39	0.85		97	0.70	0.68	-2.59		
FURNARIIDAE																		
<i>Sclerurus obscurior</i>	TI	T	47	25.36	25.07	-1.15		42	78.55	79.44	1.12		41	0.32	0.31	-3.40		
<i>Sclerurus rufigularis</i>	TI	T	150	21.02	20.73	-1.40		124	75.41	75.78	0.50		120	0.28	0.27	-3.53	▼	
<i>Sclerurus caudacutus</i>	TI	T	68	39.41	38.82	-1.50		49	90.83	91.91	1.19		46	0.44	0.43	-3.85	▼	
<i>Certhiasomus stictolaemus</i>	WO	U	201	16.90	16.35	-3.29		165	77.75	78.91	1.49		159	0.22	0.21	-6.33	▼	
<i>Deconychura longicauda</i>	WO	M	57	28.18	27.03	-4.08		48	100.19	100.66	0.47		45	0.28	0.26	-6.79	▼	
<i>Dendrocincla merula</i>	AF	NG	271	53.13	52.84	-0.56		203	105.71	105.31	-0.38		186	0.51	0.50	-2.16		
<i>Dendrocincla fuliginosa</i>	AW	U	130	40.82	39.33	-3.67		116	106.43	105.51	-0.86		109	0.39	0.37	-3.88		
<i>Glyphorhynchus spirurus</i>	WO	U	924	13.70	13.32	-2.76	▼	762	67.27	68.72	2.15	▲	732	0.21	0.19	-6.28	▼	
<i>Dendrocolaptes certhia</i>	AW	M	56	67.73	65.92	-2.68		48	125.39	124.91	-0.38		47	0.55	0.53	-3.29		
<i>Hylexetastes perrotii</i>	AW	M	47	113.37	110.09	-2.89		35	126.86	125.73	-0.89		33	0.91	0.88	-3.61		
<i>Xiphorhynchus pardalotus</i>	WO	M	355	37.83	36.38	-3.84	▼	265	101.23	101.22	-0.01		257	0.38	0.36	-5.77	▼	

<i>Campylorhamphus procurvoides</i>	WO	M	31	34.73	33.92	-2.33		27	94.20	95.22	1.09		23	0.38	0.36	-5.32	▼
<i>Xenops minutus</i>	MI	M	144	12.27	11.95	-2.62		110	64.30	64.88	0.91		103	0.19	0.18	-5.15	▼
<i>Philydor erythrocercum</i>	MI	M	85	23.70	23.60	-0.43		67	83.26	85.47	2.66		62	0.29	0.28	-3.14	
<i>Philydor pyrrhodes</i>	UI	U	28	29.69	28.92	-2.58		18	82.24	83.94	2.07		16	0.36	0.35	-3.33	
<i>Clibanornis rubiginosus</i>	NGI	NG	81	36.79	35.85	-2.56		57	80.77	80.48	-0.36		56	0.46	0.45	-2.41	
<i>Automolus ochrolaemus</i>	UI	U	35	34.49	33.15	-3.91	▼	31	85.53	86.19	0.76		28	0.40	0.38	-6.44	▼
<i>Automolus infuscatus</i>	UI	U	240	31.84	30.77	-3.35	▼	182	85.25	86.05	0.93		174	0.38	0.36	-5.57	▼
<i>Synallaxis rutilans</i>	NGI	NG	30	16.71	16.50	-1.29		23	55.35	56.35	1.80		22	0.30	0.30	-1.97	
PIPRIDAE																	
<i>Corapipo gutturalis</i>	MF	M	188	8.20	7.68	-6.34	▼	177	54.33	54.62	0.54		170	0.15	0.14	-9.09	▼
<i>Lepidothrix serena</i>	UF	U	258	10.80	10.07	-6.83	▼	203	53.09	54.13	1.95	▲	201	0.21	0.19	-9.71	▼
<i>Pseudopipra pipra</i>	UF	U	969	12.01	11.48	-4.35	▼	797	62.12	62.62	0.80	▲	774	0.20	0.18	-8.08	▼
<i>Ceratopipra erythrocephala</i>	MF	M	91	12.03	11.56	-3.96	▼	76	55.33	55.99	1.20		76	0.22	0.21	-5.91	▼
COTINGIDAE																	
<i>Lipaugus vociferans</i>	MF	M	23	71.87	67.98	-5.42		21	118.43	118.83	0.33		20	0.62	0.57	-8.19	▼
TITYRIDAE																	
<i>Schiffornis olivacea</i>	UF	U	241	34.56	32.47	-6.03	▼	173	89.66	91.00	1.49	▲	164	0.39	0.36	-9.44	▼
ONYCHORHYNCHIDAE																	
<i>Onychorhynchus coronatus</i>	UI	U	47	14.69	14.02	-4.58		33	75.92	75.51	-0.55		32	0.20	0.18	-6.12	
<i>Terentriacus erythrurus</i>	MI	M	64	6.83	6.55	-4.16		49	48.20	49.97	3.66	▲	46	0.14	0.13	-9.03	▼
<i>Myiobius barbatus</i>	MI	M	293	10.60	10.13	-4.43	▼	217	61.24	62.84	2.62	▲	204	0.18	0.16	-8.57	▼
TYRANNIDAE																	
<i>Platyrinchus saturatus</i>	NGI	NG	155	10.58	9.95	-5.92	▼	120	56.90	57.16	0.44		117	0.19	0.17	-9.47	▼
<i>Platyrinchus coronatus</i>	UI	U	219	8.75	8.29	-5.32	▼	175	53.08	53.11	0.05		165	0.17	0.15	-8.33	▼
<i>Platyrinchus platyrhynchos</i>	UI	U	22	12.19	11.51	-5.60	▼	18	61.84	62.60	1.21		18	0.20	0.18	-10.40	▼
<i>Corythopsis torquatus</i>	NGI	NG	170	14.75	14.55	-1.38		112	63.62	63.58	-0.06		109	0.24	0.23	-4.64	▼
<i>Mionectes macconnelli</i>	MF	M	647	12.48	11.83	-5.19	▼	500	62.97	63.10	0.21		483	0.20	0.19	-7.92	▼
<i>Rhynchocyclus olivaceus</i>	MI	M	47	19.38	19.12	-1.33		39	69.80	70.40	0.87		37	0.29	0.27	-6.51	▼
<i>Attila spadiceus</i>	MI	M	26	33.27	31.75	-4.58		27	81.48	81.36	-0.15		26	0.41	0.39	-6.04	▼



<i>Rhytipterna simplex</i>	MI	M	24	34.44	32.29	-6.22	▼	25	95.33	95.39	0.07	24	0.37	0.34	-7.40	▼	
VIREONIDAE																	
<i>Tunchiornis ochraceiceps</i>	UI	U	225	10.32	9.63	-6.67	▼	172	56.52	56.17	-0.62	163	0.19	0.17	-8.60	▼	
TROGLODYTIDAE																	
<i>Microcerculus bambla</i>	NGI	NG	72	16.72	16.11	-3.65		53	54.59	55.70	2.04	48	0.31	0.29	-7.07	▼	
<i>Cyphorhinus arada</i>	TI	T	172	20.34	19.22	-5.50	▼	122	58.87	60.30	2.43	▲	109	0.35	0.31	-10.29	▼
POLIOPTILIDAE																	
<i>Microbatas collaris</i>	NGI	NG	272	10.84	10.48	-3.26	▼	200	49.53	50.43	1.81	▲	190	0.22	0.21	-7.62	▼
TURDIDAE																	
<i>Turdus albicollis</i>	UF	U	335	50.05	46.61	-6.87	▼	234	102.09	102.80	0.69	226	0.50	0.45	-9.68	▼	
PARULIDAE																	
<i>Myiothlypis rivularis</i>	RI	NG	21	13.31	12.34	-7.30		21	61.70	60.97	-1.18	18	0.22	0.20	-8.68		
CARDINALIDAE																	
<i>Cyanoloxia rothschildii</i>	UF	U	61	25.75	24.58	-4.55		49	75.49	77.96	3.27	47	0.34	0.32	-7.87	▼	
THRAUPIDAE																	
<i>Tachyphonus surinamus</i>	MF	M	174	20.69	19.84	-4.11	▼	141	79.54	78.51	-1.30	139	0.27	0.25	-5.26	▼	
<i>Lanio fulvus</i>	MI	M	29	25.88	25.37	-1.97		21	89.66	88.47	-1.33	21	0.30	0.29	-5.00		

Guild: AW=ant-woodcreeper, AF=army-ant follower, GI=gap insectivore, HU=hummingbird, MF=midstory frugivore, MI=midstory insectivore, NGI=near-ground insectivore, RI=riparian insectivore, TI=terrestrial insectivore, UF=understory frugivore, UI=understory insectivore, WO=woodcreeper

Stratum: M=midstory, U=understory, NG=near-ground, T=terrestrial

▼=decreasing with 95% credible intervals entirely negative, ▲=increasing with 95% credible intervals entirely positive